Stem Cell Reports
Article

ISSCR

OPEN ACCESS

Long-Term Culture of Self-renewing Pancreatic Progenitors Derived from Human Pluripotent Stem Cells

Jamie Trott,[1,*] Ee Kim Tan,[1] Sheena Ong,[1] Drew M. Titmarsh,[1,6] Simon L.I.J. Denil,[1] Maybelline Giam,[1] Cheng Kit Wong,[1] Jiaxu Wang,[2] Mohammad Shboul,[1] Michelle Eio,[1] Justin Cooper-White,[3] Simon M. Cool,[1] Giulia Rancati,[1] Lawrence W. Stanton,[2] Bruno Reversade,[1] and N. Ray Dunn[1,4,5,*]

[1]Institute of Medical Biology, Agency for Science Technology and Research (A*STAR), 8a Biomedical Grove, #06-06 Immunos, Singapore 138648, Singapore
[2]Genome Institute of Singapore, Agency for Science Technology and Research (A*STAR), 60 Biopolis Street, #02-01, Singapore 138672, Singapore
[3]Australian Institute for Bioengineering and Nanotechnology, The University of Queensland, St Lucia, QLD 4072, Australia
[4]Lee Kong Chian School of Medicine, Nanyang Technological University, 50 Nanyang Avenue, Singapore 639798, Singapore
[5]School of Biological Sciences, Nanyang Technological University, 60 Nanyang Drive, Singapore 637551, Singapore
[6]Present address: Scaled Biolabs Inc., 479 Jessie Street, San Francisco, CA 94103, USA
*Correspondence: jamie.trott@imb.a-star.edu.sg (J.T.), ray.dunn@imb.a-star.edu.sg (N.R.D.)
http://dx.doi.org/10.1016/j.stemcr.2017.05.019

SUMMARY

Pluripotent stem cells have been proposed as an unlimited source of pancreatic β cells for studying and treating diabetes. However, the long, multi-step differentiation protocols used to generate functional β cells inevitably exhibit considerable variability, particularly when applied to pluripotent cells from diverse genetic backgrounds. We have developed culture conditions that support long-term self-renewal of human multipotent pancreatic progenitors, which are developmentally more proximal to the specialized cells of the adult pancreas. These cultured pancreatic progenitor (cPP) cells express key pancreatic transcription factors, including PDX1 and SOX9, and exhibit transcriptomes closely related to their in vivo counterparts. Upon exposure to differentiation cues, cPP cells give rise to pancreatic endocrine, acinar, and ductal lineages, indicating multilineage potency. Furthermore, cPP cells generate insulin+ β-like cells in vitro and in vivo, suggesting that they offer a convenient alternative to pluripotent cells as a source of adult cell types for modeling pancreatic development and diabetes.

INTRODUCTION

The adult pancreas comprises three major lineages: endocrine, acinar, and ductal (Pan and Wright, 2011). The endocrine compartment resides in the islets of Langerhans and consists of cells that secrete hormones required for the maintenance of euglycemia, including α cells that secrete glucagon and β cells that secrete insulin and whose failure leads to diabetes. Acinar cells produce digestive enzymes and, together with duct cells, form the exocrine pancreas. Development of the human pancreas begins with the emergence of the dorsal and ventral pancreatic buds from the posterior foregut at Carnegie stage (CS) 12 (Jennings et al., 2015; Shih et al., 2013). These rudimentary structures consist of multipotent pancreatic progenitors that proliferate extensively and undergo branching morphogenesis before fusing to form the pancreatic anlage. Each of the three major pancreatic lineages is derived from these progenitor cells following a series of cell-fate decisions and morphological changes.

In the developing foregut, transcription factor expression patterns demarcate regions that give rise to specific organs, such as the pancreas and liver. In the mouse, the transcription factor PDX1 is expressed in the emerging pancreatic buds and the neighboring antral stomach and rostral intestine (McCracken et al., 2014), and is absolutely required for pancreatic development (Jonsson et al., 1994; Offield et al., 1996). Expression of SOX9, which marks proliferative cells in a variety of tissues, distinguishes PDX1+ cells that will form the pancreas from those that give rise to other tissues (Shih et al., 2015). Expression of NKX6-1 follows that of PDX1 and SOX9 and, in humans, is required prior to transient activation of NGN3 for the generation of mature, functional β cells (Nostro et al., 2015; Russ et al., 2015). Finally, RFX6, FOXA2, and members of the GATA and HNF transcription factor families are expressed dynamically following specification of the definitive endoderm and throughout development of the pancreas (Conrad et al., 2014). Immunohistochemistry of human embryos at sequential stages during early pancreatic development suggests that the tissue specificity of these transcription factors is similar between mice and humans, although there appear to be differences in when they are expressed (Jennings et al., 2013, 2015).

A series of genetic studies in mice led to the identification of numerous signaling pathways that regulate pancreatic development (Shih et al., 2013), thereby inspiring the development of protocols for the generation of pancreatic progenitors (Kroon et al., 2008) and subsequently β-like cells from human pluripotent stem cells (Pagliuca et al., 2014; Rezania et al., 2014; Russ et al., 2015). The ultimate goal of these studies is to generate functional β cells capable of maintaining euglycemia and alleviating diabetes. However, these protocols are technically challenging and

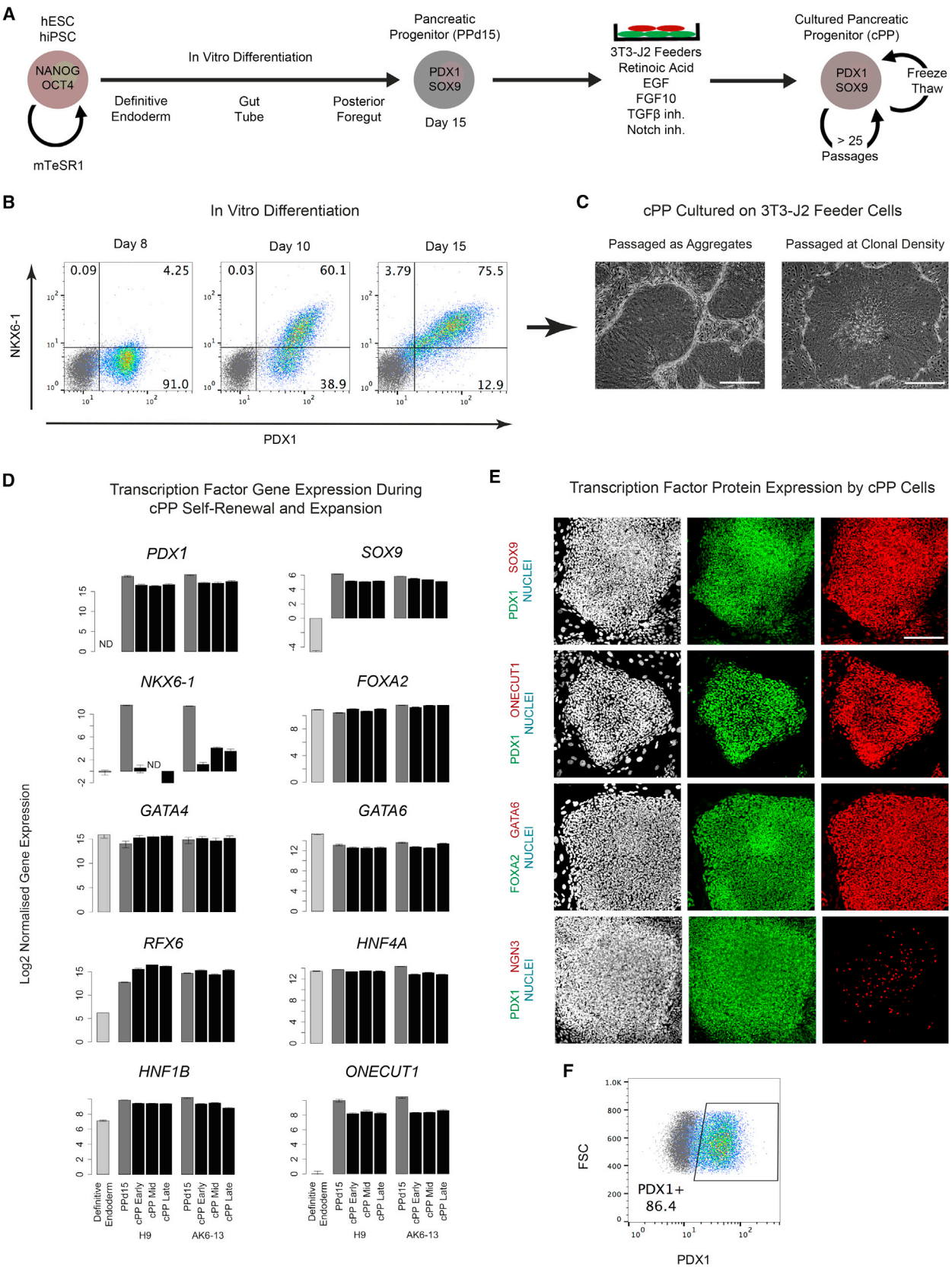

(legend on next page)

expensive to conduct, often resulting in low differentiation efficiencies, partly due to the variability inherent in long, multi-step differentiation protocols that seek to recapitulate the entire developmental history of a β cell. These issues are exacerbated when such protocols are applied to genetically diverse human embryonic stem cells (hESCs) and induced pluripotent stem cells (hiPSCs). A potential solution is to initiate differentiation from an alternative cell type that is developmentally more proximal to the β cell. The obvious candidate is the PDX1+SOX9+ progenitor cell population of the emerging pancreatic bud that is capable of extensive proliferation and gives rise to all of the mature functional cells of the pancreas.

We describe a cell culture platform that enables hESC- and hiPSC-derived pancreatic progenitors to be captured and expanded in vitro. These cultured pancreatic progenitor (cPP) cells express key pancreatic transcription factors, including PDX1 and SOX9, and are stable for >25 passages. Crucially, cPP cells are closely related to their in vivo counterparts at the transcriptome level and can be differentiated into cells of the endocrine, acinar, and ductal lineages. Therefore, cPP cultures represent a convenient alternative system for studying pancreatic development that circumvents the need to repeatedly generate progenitors from pluripotent cells by directed differentiation. Finally, replacing heterochronic differentiation cultures with comparatively stable and homogeneous cPP cultures will facilitate the development of more robust protocols for the generation of pancreatic cell types from genetically diverse patient-specific hiPSC lines.

RESULTS

Maintenance and Expansion of cPP Cells Derived from hESCs and hiPSCs

Directed differentiation guided by growth factors and small molecules facilitates the generation of diverse cell types from pluripotent stem cells. We chose to produce pancreatic progenitors from hESCs and hiPSCs (Figure S1) using reagents based on the early stages of a protocol designed to generate mature β cells (Figure S2A; Rezania et al., 2014). This differentiation strategy induced the sequential expression of PDX1 followed by NKX6-1 and yielded a median of 80% PDX1+NKX6-1+ cells after 15 days (PPd15 cells; Figures 1B and S2C). However, as is often observed during directed differentiation from pluripotent cells, the kinetics of PDX1 and NKX6-1 expression varied between cell lines (Figure S2B) (Cahan and Daley, 2013). Therefore, we sought to capture, synchronize, and expand PPd15 cells in culture.

The 3T3-J2 mouse embryonic fibroblast cell line has been used to culture progenitor cells derived from a variety of human tissues, including endoderm-derived intestinal stem cells (Rheinwald and Green, 1975a, 1975b; Wang et al., 2015). We therefore determined whether pancreatic progenitor cells could be similarly expanded, if provided with appropriate stimuli. We tested a series of signaling agonists and inhibitors previously shown to regulate pancreatic development, including EGFL7, BMP4, nicotinamide, LIF, WNT3A, R-Spondin-1, Forskolin (cAMP agonist), GSK3β inhibition (CHIR99021), and inhibitors of BMP (LDN-193189) and SHH (KAAD-cyclopamine) signaling. Ultimately, a combination of EGF, retinoic acid, and inhibitors of transforming growth factor β (TGF-β, SB431542) and Notch signaling (DAPT) was found to support long-term self-renewal of pancreatic progenitors (Figure 1A). To establish stable cPP cell lines, PPd15 cells were replated on a layer of 3T3-J2 feeder cells in the presence of these factors. Thereafter, cPP cells were routinely passaged once weekly as aggregates at an average split ratio of 1:6, although they were also capable of forming colonies at clonal density (Figure 1C). This suggests a doubling time of ~65 hr in culture, similar to the 61 hr we routinely observe for hESCs when cultured on a layer of mouse embryonic fibroblasts.

We were able to generate self-renewing cPP cell lines from four different genetic backgrounds using two hESC (H9 and HES3) and three hiPSC cell lines (AK5-11, AK6-8, and AK6-13 derived in house); these diverse cPP cells expressed comparable levels of genes encoding key pancreatic transcription factors, including *PDX1* and *SOX9* (Figure S2D). Two cPP cell lines selected for further analysis (H9#1 and

Figure 1. Derivation of cPP Cell Lines from hESC and hiPSC

(A) Pancreatic progenitors generated after 15 days of differentiation using the STEMdiff directed differentiation kit (PPd15 cells) were plated and expanded on a layer of 3T3-J2 feeder cells in medium supplemented with the indicated growth factors and signaling inhibitors.

(B) Intracellular flow cytometric analysis for PDX1 and NKX6-1 at days 8, 10, and 15 of differentiation using H9 hESCs.

(C) Phase-contrast images of cPP cells passaged as aggregates (left) and as single cells (right). Scale bar, 100 μm.

(D) Gene expression measured by qRT-PCR using samples harvested from PPd15 cells and cPP cells at early (6–8), middle (11–13), and late (14–18) passages. Cells were derived from both AK6-13 hiPSC and H9 hESC. Gene expression in definitive endoderm (H9 hESCs after 4 days STEMdiff differentiation) is shown for comparison. Values are plotted on a $\log_2$ scale and error bars represent the SE of three technical replicates. ND, not detected.

(E) Immunofluorescence staining of cPP cells for key pancreatic transcription factors. Scale bar, 100 μm.

(F) Intracellular flow cytometric analysis of cPP cells for PDX1. Gray dots represent control cells stained with isotype control antibodies.

A

Chromosome Counting

cPP Cell Line	H9 Pedigree #1	H9 Pedigree #1	H9 Pedigree #1	H9 Pedigree #2	H9 Pedigree #3	AK6_13	AK6_13	AK6-8
Pluripotent Cells	hESC	hESC	hESC	hESC	hESC	iPSC	iPSC	iPSC
cPP Passage	8	13	19	12	15	6	11	12
Spread Count	50	50	51	50	50	50	50	50
<40	0	2	0	0	0	0	0	0
40	0	0	0	2	0	2	0	0
41	0	4	0	0	0	2	0	0
42	0	0	0	0	0	0	2	0
43	0	0	0	0	0	4	4	2
44	0	6	0	2	2	0	0	0
45	4	4	0	6	0	0	6	4
46	80	28	5.9	86	96	84	80	88
47	10	52	94.1	2	2	8	6	6
48	4	0	0	2	0	0	0	0
49	2	2	0	0	0	0	0	0
50	0	2	0	0	0	0	0	0
>50	0	0	0	0	0	0	2	0

B

M-FISH Analysis of Chromosomal Translocations
AK6-13 cPP Passage 20

46, XY - No structural abnormalities detected [19/20 Spreads]

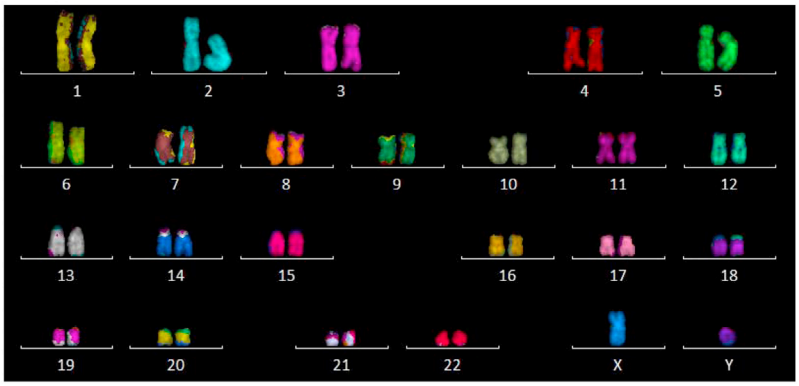

Figure 2. Chromosome Counting and M-FISH Analysis Reveals cPP Cells Are Genetically Stable

(A) Chromosome counting of cPP cells from diverse genetic backgrounds at different passage numbers. Values shown are the percentage of spreads with a given number of chromosomes, with the modal chromosome count for each cPP line highlighted. A modal (shared by >80% of cells) chromosome number of 46 is indicative of a normal karyotype and of karyotypic stability. Five out of six cPP cell lines analyzed exhibited a modal chromosome count of 46 after >6 passages, without evidence of fragments or dicentric chromosomes, and are considered karyotypically stable. In H9 pedigree #1, cells gradually acquired an additional isochromosome upon passaging. Traditional G-band karyotyping (data not shown) subsequently found this to be i(12) (p10)[20], an isochromosome commonly observed in hESC cultures.

(B) Multicolor fluorescence in situ hybridization (M-FISH) enables the detection of chromosomal structural abnormalities at significantly higher resolution than chromosome counting alone. M-FISH of passage 20 AK6-13 cPP cells failed to detect aneuploidy, translocations or deletions in 19/20 spreads analyzed. A representative image of a single chromosome spread is shown.

AK6-13) have been maintained in culture for >20 passages to date enabling $>10^{18}$-fold expansion over 20 weeks. Crucially, cPP cells can be frozen and thawed with no apparent loss of proliferation or viability, suggesting cPP cells could replace pluripotent cells as a starting point for further differentiation to mature pancreatic cell types such as insulin-secreting β cells.

To determine whether cPP cultures consist of a stable and homogeneous population of cells, we measured the expression of key pancreatic transcription factors at the mRNA and protein levels. Gene expression of numerous markers of pancreatic bud cells, including *PDX1* and *SOX9*, remained constant over extended periods in culture, indicating that our culture conditions maintain a stable population of pancreatic progenitors (Figure 1D). To determine whether cPP cultures represent a homogeneous population, we carried out immunostaining for a selection of pancreatic markers and found these to be expressed near ubiquitously at the protein level (Figure 1E). Furthermore, flow cytometric analysis showed that approximately 85% of cPP cells were PDX1+ (Figure 1F).

However, *NKX6-1* expression was rapidly downregulated in culture, and NKX6-1 protein was not detected by immunostaining. Furthermore, we were able to establish cPP cell lines from day 7, 10, and 15 differentiation cultures (data not shown), the earliest time point being prior to expression of *NKX6-1* and suggesting that cPP culture conditions stabilize pancreatic progenitors in a developmental state that precedes *NKX6-1* activation. Very few cells were NGN3+, which marks early endocrine progenitors, indicating that differentiation was blocked at the progenitor stage under our culture conditions. Finally, chromosome counting showed that five out of six cPP cells carried 46 chromosomes without signs of structural changes, such as presence of fragments or dicentric chromosomes (Figure 2A). Multiplex fluorescence in situ hydridization (M-FISH) analysis on the AK6-13 line at passage 20 confirmed the absence of karyotypic abnormalities (Figure 2B). Collectively, these data demonstrate that our cPP culture conditions capture pancreatic progenitors as a near homogeneous population that is maintained stably over extended periods of time and is capable of extensive expansion.

Transcriptome Analysis Demonstrates cPP Cells Are Closely Related to Their In Vivo Counterparts

We next determined the transcriptome-wide gene counts by RNA-seq for cPP lines from three different genetic backgrounds and the PPd15 differentiation cultures from which they were established. Samples for RNA-seq were also taken from cPP cells at early, mid, and late passages. Gene

expression levels correlated strongly between different cPP samples, indicating that neither genetic background nor time in culture significantly affect the cPP transcriptome (Figure S3A). However, to completely eliminate donor-specific effects on gene expression, the following analysis used mean gene counts for cPP (early passage) and PPd15 cells derived from H9 and HES3 hESCs and AK6-13 hiPSCs.

To determine how similar cPP cells are to their in vitro and in vivo counterparts, we compared the cPP transcriptome with the published transcriptomes of pancreatic progenitors differentiated in vitro (Cebola PP) and from CS16-18 human embryos (CS16-18 PP), as previously described (Cebola et al., 2015), and a diverse collection of adult and embryonic tissues (Bernstein et al., 2010; Petryszak et al., 2013). Relative to non-pancreatic tissues, cPP cells exhibited similar patterns of gene expression to both PPd15 and Cebola PP cells (Figure 3A). Furthermore, cPP, PPd15, and Cebola PP cells closely resembled in vivo pancreatic progenitors at CS16-18, and all four cell populations expressed similar levels of genes associated with endodermal and pancreatic development (Figure 3B). However, as expected, cPP cells do not express the late-stage pancreatic progenitor markers *NKX6-1*, *PTF1A*, and *CPA1*. When taken together, these data demonstrate that the culture conditions described here maintain cPP cells in a developmental state closely related to both the embryonic human pancreas and pancreatic progenitors generated by directed differentiation.

To further characterize the transcriptional identity of cPP cells, we sought to identify genes that distinguish them from other lineages. Specifically expressed genes were defined as those that are variably expressed across the aforementioned panel of 25 tissues (coefficient of variance >1) and whose expression is upregulated in cPP cells (Z score >1), as previously described (Cebola et al., 2015). In total 1,366 genes were identified, including numerous well-characterized markers of pancreatic progenitor cells, such as *PDX1*, *SOX9*, *MNX1*, and *RFX6* (Figure 3C). To confirm the validity of this method, we demonstrated that these genes are not expressed by other endodermal derivatives, including liver, colon, and lung (Figure S3B). Encouragingly, around 80% of genes specifically expressed by cPP cells were shared with CS16-18 pancreatic progenitors and/or PPd15 cells. Furthermore, gene Z scores were highly correlated between these three pancreatic cell types but not with liver (Figure S3C), further demonstrating the transcriptional similarities between cPP cells and other pancreatic progenitors.

To determine the functional roles of cPP-specific genes, we analyzed associated Gene Ontology (GO) terms. The most enriched terms were those associated with endocrine pancreas development (Figure 3D, above). In order to determine how our culture conditions affect the behavior of cPP cells, we analyzed GO terms associated with genes expressed by cPP cells but not PPd15 or CS16-18 pancreatic progenitor cells (Figure 3D, below). Interestingly, the most enriched terms were those associated with aspects of cell division and telomere maintenance. Indeed, genes associated with these enriched terms, such as those encoding telomerase reverse transcriptase (*TERT*) and proliferating cell nuclear antigen (*PCNA*), were consistently upregulated in cPP cells from different genetic backgrounds, compared with the PPd15 populations from which they were derived (Figures 3E and 3F). We conclude that our feeder-based culture system maintains pancreatic progenitors as a stable population while upregulating genes required for long-term self-renewal.

A Feeder Layer of 3T3-J2 Cells Prevents cPP Differentiation while Exogenous Signals Promote Proliferation

We next investigated the roles played by the individual components of our culture system, specifically the layer of irradiated 3T3-J2 feeder cells, stimulation with EGF, FGF10, and retinoic acid (RA), and inhibition of the TGFβ and Notch signaling pathways. To assess the importance of the feeder layer, cPP cells were subcultured onto a layer of 3T3-J2 cells plated at decreasing densities and maintained in complete cPP culture media for 7 days. At reduced feeder densities, cPP cells continued to proliferate rapidly but quickly altered their morphology and could not be serially passaged (Figure 4A). The levels of *PDX1* and *SOX9* remained stable, indicating cPP cells are committed to the pancreatic lineage, while markers of duct (*KRT19* and *CA2*) and acinar (*CPA1* and *AMY2B*) differentiation were upregulated (Figure 4B). However, we did not observe upregulation of endocrine markers (*NGN3* and *NKX2-2*), suggesting that 3T3-J2 feeder cells are required to block further differentiation toward the ductal and acinar linages.

To establish the roles played by the growth factors and small molecules in our culture media, we removed each individually and assessed the effect on differentiation and proliferation. Exclusion of EGF or RA prevented cPP expansion, while removal of the TGF-β inhibitor SB431542 caused colonies to detach from the feeder layer (Figure 4C). Removal of either FGF10 or the γ-secretase inhibitor DAPT did not significantly affect colony size or morphology in the short term but, when removed from the culture media over multiple passages, led to a noticeable loss of viability. Interestingly, none of the growth factors or signaling inhibitors was individually required for maintenance of *PDX1* or *SOX9* expression (Figure 4D). Indeed, removal of RA actually increased *PDX1* expression. These results suggest that the growth factors and inhibitors present in our culture media are primarily required to drive proliferation of cPP cells rather than maintain their developmental state.

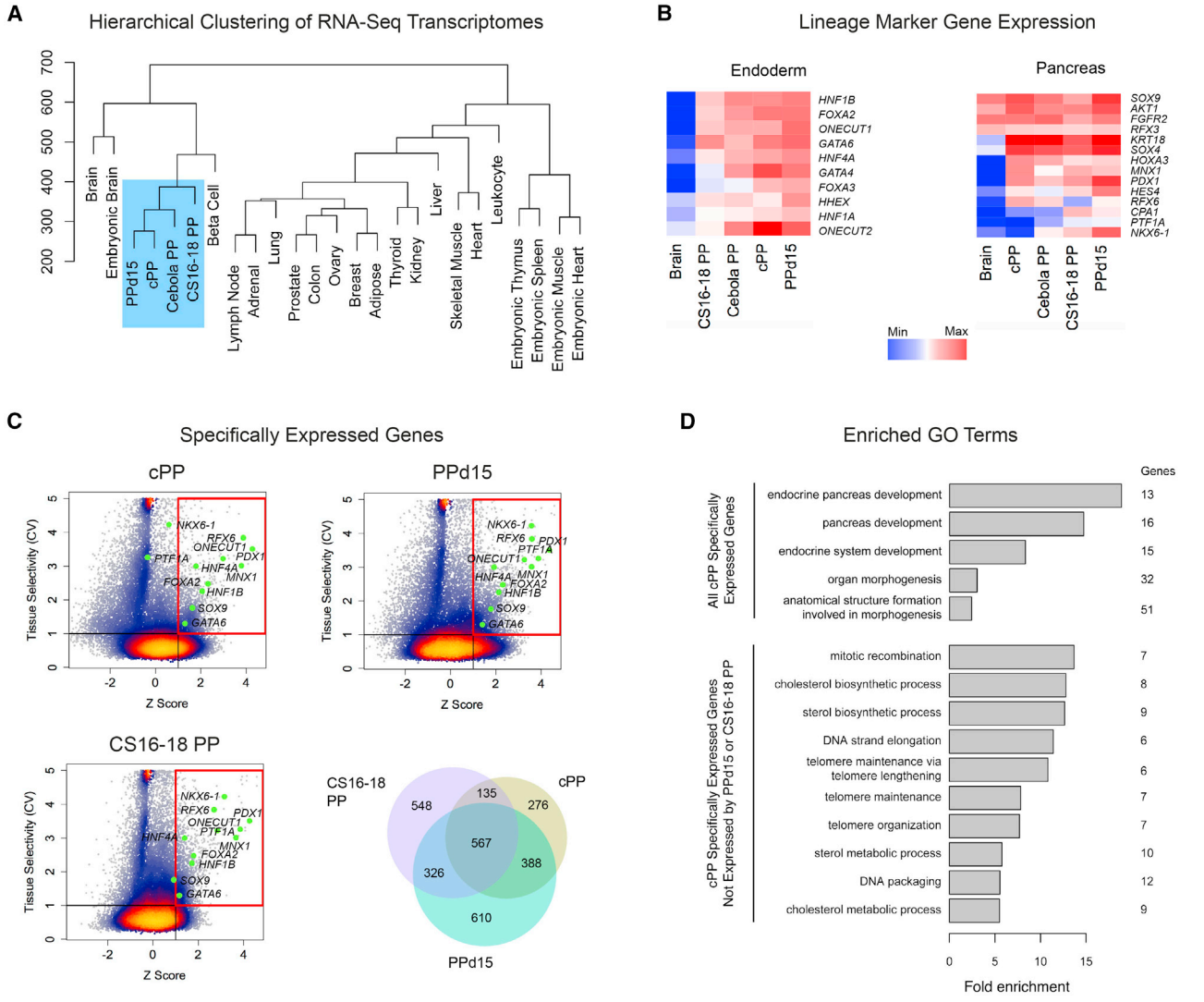

(legend on next page)

To quantify the effect of exogenous signaling molecules on the maintenance and expansion of cPP cells, we used a microbioreactor array (MBA) screening platform to measure differentiation and proliferation (Titmarsh et al., 2012). Single cPP cells were seeded in Matrigel-coated culture chambers in the absence of feeders and exposed for 3 days to complete cPP culture media in which the levels of EGF, RA, and DAPT were varied (Figure S4). We then used an image-segmentation algorithm to identify individual nuclei and quantify immunofluorescence staining for PDX1 and SOX9, thereby enabling us to determine the percentage of double-positive cells following exposure to different growth factor regimes. Reducing the levels of any of the three factors led to a reduction in both the total number of cells and the number of PDX1+SOX9+ cells (Figure 4E). However, neither the mean levels of PDX1/SOX9 nor the percentage of PDX1+SOX9+ cells were dependent on the levels of these factors, suggesting they act primarily as mitogens. Interestingly, we noticed an increase in the number and percentage of PDX1+SOX9+ cells, but no change in the overall proliferation rate, when cells were exposed to higher concentrations of autocrine signals, particularly when provided with maximal levels of EGF, RA, and DAPT (Figure S4D). Exposure to endogenous soluble signaling molecules is therefore required to maintain PDX1 and SOX9 independently of proliferation.

When taken together, these observations demonstrate that self-renewal of cPP cells is dependent on activation of the EGF, FGF10, and RA pathways and inhibition of Notch signaling. Indeed, cPP cells and their in vitro (PPd15) and in vivo (CS16-18 pancreatic progenitor) equivalents expressed high levels of multiple receptors of EGF, FGF, RA, and Notch signaling, as well as the TGFβ receptors ALK4 and ALK5 (encoded by *ACVR1B* and *TGFBR1*, respectively) that are inhibited by SB431542 (Figure 4F). Consistent with our observations, production of FGF10 and RA by the surrounding mesenchyme is essential for expansion of the murine pancreatic bud (Bhushan et al., 2001; Martín et al., 2005; Ye et al., 2005), while EGFR is expressed throughout the pancreas and regulates islet development (Miettinen et al., 2000). Intracellular Notch signaling promotes expansion of pancreatic progenitors and prevents their further differentiation into endocrine cells (Hald et al., 2003; Murtaugh et al., 2003). Therefore, our observation that the γ-secretase inhibitor DAPT promotes proliferation of cPP cells is somewhat surprising. However, FGF10 has been shown to promote Notch activity in the developing pancreatic epithelium (Hart et al., 2003), and cPP cells express intermediate levels of the Notch effector *HES1* relative to the 23 tissues described in Figure 3A (data not shown). Therefore, the relatively low concentration of DAPT added to cPP cultures most likely serves to temper Notch activity, and exceptionally high levels of Notch activity might actually suppress proliferation.

Differentiation of cPP Cells into Pancreatic Cell Types In Vitro and In Vivo

The canonical property of pancreatic progenitors is their ability to differentiate into each of the three lineages that constitute the pancreas as well as their functional derivatives. Initially, we sought to determine whether cPP cells are capable of commitment to the endocrine, duct, and acinar lineages in vitro. Since robust protocols for the directed differentiation of pancreatic duct and acinar cells have yet to be developed, cPP cells were replated in the absence of feeders and exposed to a minimal signaling regime that promotes multilineage differentiation (Figure 5A). Over the course of 12 days, we observed

Figure 3. Transcriptome Analysis of cPP Cells by RNA-Seq

(A) Hierarchical clustering of Euclidean distances between transcriptomes of diverse adult and embryonic tissues shows that in vitro and in vivo pancreatic progenitors exhibit similar patterns of gene expression. Log_2-transformed gene count values were used to calculate Euclidian distances. For detailed information on the sources of data used here, see Table S1.

(B) Heatmaps showing log_2-transformed gene expression levels of key endodermal and pancreatic markers by in vitro and in vivo pancreatic progenitors. Levels in brain are shown for comparison.

(C) Genes specifically expressed by cPP, PPd15, and CS16-18 pancreatic progenitors. The coefficient of variance (CV) for each protein-coding gene across the 25 tissues shown in (A) was plotted against the corresponding *Z* score (see Supplemental Experimental Procedures). Specifically expressed genes are located in the upper right-hand quadrant (CV >1 and *Z* score >1) and include genes with well-characterized roles in early pancreatic development (labeled). The color scale denotes the number of genes. The Venn diagram shows overlap between genes specifically expressed by cPP, PPd15, and CS16-18 pancreatic progenitors.

(D) Biological process Gene Ontology (GO) terms associated with all genes specifically expressed by cPP cells (above) or genes specifically expressed by cPP cells but not PPd15 or CS16-18 pancreatic progenitors (below). Only GO terms associated with >5 genes and/or an adjusted p value <0.01 are shown.

(E) Heatmap of expression levels of genes associated with the enriched GO terms mitotic recombination, DNA strand elongation, telomere maintenance, and DNA packaging. Levels are shown for individual cPP and PPd15 populations derived from three different genetic backgrounds (H9, AK6-13, and HES3) relative to the maximum detected value across the 25 different tissues shown in (A).

(F) Expression of selected telomerase pathway genes as measured by qRT-PCR in cPP and PPd15 cells. Error bars represent the SE of three technical replicates.

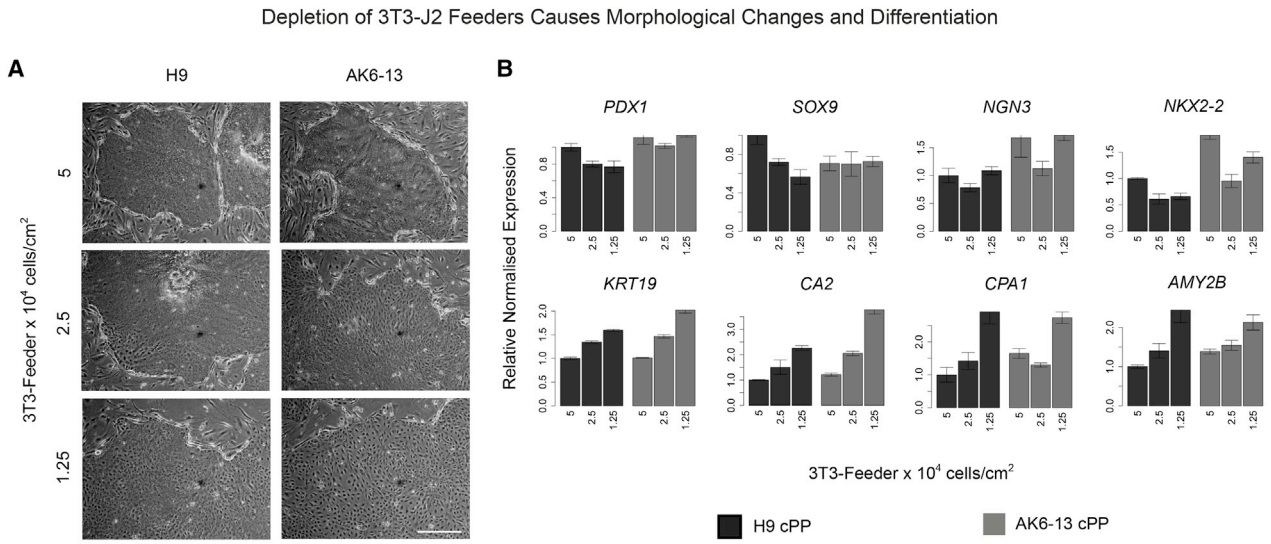

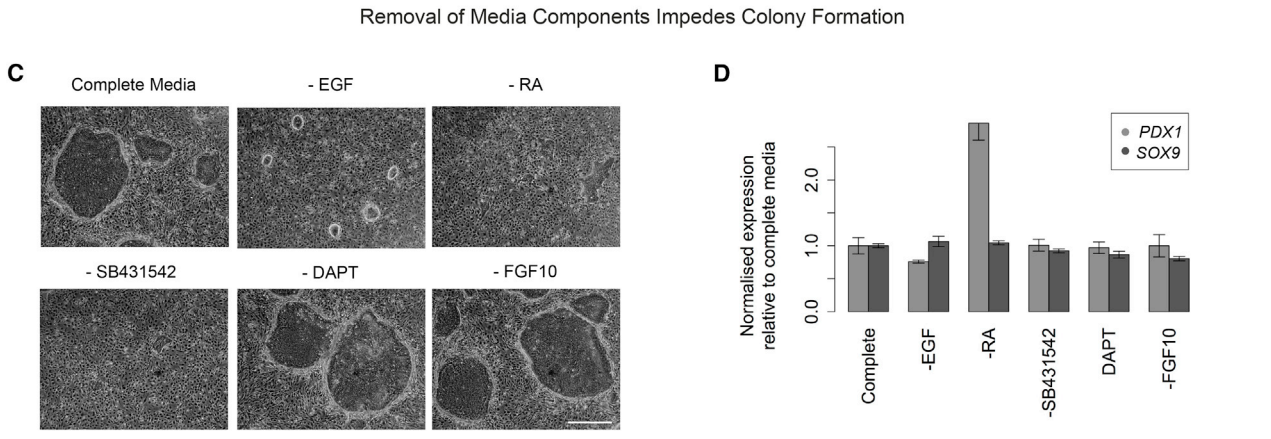

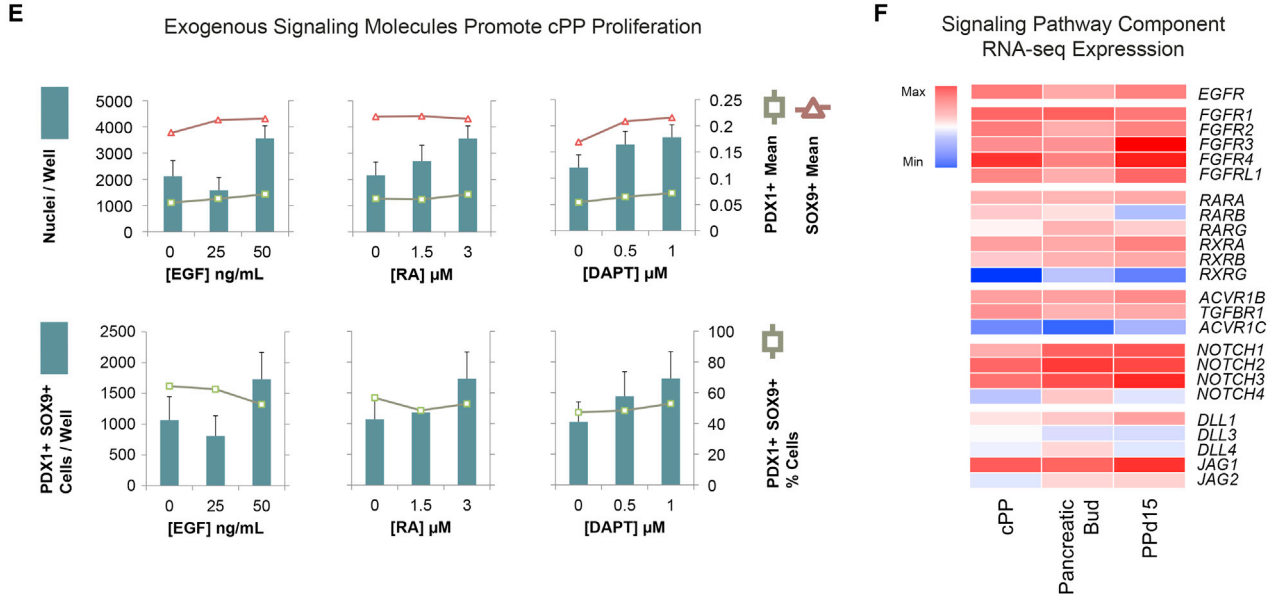

(legend on next page)

upregulation of endocrine (*NKX6-1*, *INS*, and *GCG*), acinar (*CPA1*, *AMY2B*, and *TRYP3*), and duct (*SOX9*, *KRT19*, and *CA2*) markers, demonstrating that cPP cells retain multilineage potency in vitro (Figure 5B).

Of particular interest is the ability to generate β-like cells capable of secreting insulin in response to elevated glucose levels. Several groups recently published protocols that describe the differentiation of particular hESC and hiPSC cell lines into β-like cells. Activation of NKX6-1 prior to expression of NGN3 is thought to be essential for the formation of mature, functional β cells (Nostro et al., 2015; Russ et al., 2015). Therefore, we selected the four most promising protocols and assessed their ability to induce *NKX6-1* expression while maintaining low levels of *NGN3* (Pagliuca et al., 2014; Rezania et al., 2014; Russ et al., 2015; Zhang et al., 2009). Specifically, cPP cells were cultured as monolayers or aggregates, then exposed to the section of each differentiation protocol shown to induce NKX6-1 expression (Figure S5A). The protocol described by Russ et al. (2015) produced the highest levels of *NKX6-1* expression and minimal activation of *NGN3*, with monolayer and suspension cultures yielding a very similar response (Figure S5B). Since the original protocol demonstrated the generation of insulin-secreting β-like cells when cells were differentiated as aggregates, we chose to use the 3D suspension platform for subsequent experiments.

Using the Russ et al. (2015) protocol, we found that around 40% of cPP cells reactivate NKX6-1. However, doubling the length of each of the first two treatments enabled the generation of nearly 70% double-positive cells, similar to the number originally reported (Figures 5E, S5C, and S5D). Interestingly, these PDX1+NKX6-1+ cells generated convoluted structures reminiscent of the branching morphogenesis of the embryonic pancreas (Figures 5D and 5F). Further differentiation induced expression of the endocrine markers NKX2-2 and NGN3, the latter in a smaller subset of cells, reflecting its transient expression during endocrine commitment (Schwitzgebel et al., 2000; Figure 5G). Finally, after 16 days, 20% of cells contained C-peptide, a proxy for insulin production, similar to the 25% reported by Russ et al. (2015). Crucially, C-peptide+ cells did not co-express the α cell hormone glucagon, suggesting that these cells are unlike the polyhormonal cells produced by earlier generations of protocols, which are unable to secrete insulin in response to elevated glucose levels. However, *NGN3* levels remained high at the end of the protocol and *INS* mRNA levels were significantly lower than in isolated human islets, suggesting that further optimization of the protocol is required (Figure 5K).

The most stringent test of developmental potency is whether a progenitor can differentiate into a particular lineage in vivo. To assess the potency of cPP cells, we injected these cells under the renal capsules of immunodeficient mice and immunostained for markers of the three major pancreatic lineages after >23 weeks. We were able to identify large areas of cells expressing the β-cell marker C-peptide as well as the duct marker keratin 19 (KRT19), but we were unable to find trypsin+ acinar cells or glucagon+ endocrine cells (Figure 5L). However, trypsin+ cells were also observed rarely by Rezania et al. (2014) following transplantation of pancreatic progenitors, possibly because acinar cells cannot survive in the absence of ducts to carry away the digestive enzymes they secrete. The absence of cells expressing glucagon was surprising, but likely reflects generation of C-peptide+ cells by default in the absence of inductive signals required to form glucagon+ α cells.

The C-peptide+ cells did not form classical islet-like structures, but instead formed a series of interconnected cystic structures, as others have observed previously (Rostovskaya et al., 2015). Furthermore, we did not observe expansion of the progenitor population once transplanted, suggesting cPP cells differentiate rapidly into less proliferative cells

Figure 4. A Layer of 3T3-Feeder Cells and Exogenous Signaling Molecules Are Required for the Maintenance and Expansion of cPP Cells

(A) Phase-contrast images of H9 and AK6-13 cPP cells after 7 days culture in complete medium on 3T3-feeder cells plated at densities of 5×10^4, 2.5×10^4, and 1.25×10^4 cells/cm^2. Scale bar, 100 μm.

(B) Gene expression measured by qRT-PCR for samples harvested from cultures in (A) for endocrine (*NGN3* and *NKX2-2*), ductal (*KRT19* and *CA2*), and acinar (*CPA1* and *AMY2B*) marker genes. Error bars represent the SE of three technical replicates.

(C) Phase-contrast images of cPP cells cultured for 6 days in complete medium with individual components omitted. Scale bar, 100 μm.

(D) *PDX1* and *SOX9* expression measured by qRT-PCR for samples harvested in (C). Error bars represent the SE of three technical replicates.

(E) Microbioreactor array (MBA) screening of factors required to propagate PDX1+SOX9+ cPP cells. Effects of reducing or removing selected factors (EGF, RA, DAPT) from complete medium containing all factors at the following levels: EGF (50 ng/mL), RA (3 μM), DAPT (1 μM), SB431542 (10 μM), and FGF10 (50 ng/mL). Top panels: effects on total nuclei per chamber, and PDX1 and SOX9 mean nuclear intensity. Lower panels: effects on the total number of PDX1+SOX9+ cells per chamber and percentage of PDX1+SOX9+ cells. Data represent the mean of ten chambers within a column treated with the given condition ± the SE.

(F) Heatmap showing RNA-seq expression levels of components of signaling pathways that regulate cPP proliferation: EGF (*EGFR*), FGF10 (*FGFR1-4*, *6* and *FGFRL2*), RA (*RARA*, *RARB*, *RARG*, *RXRA*, *RXRB*, and *RXRG*), SB431542 (*ACVR1B* [ALK4], *TGFBR1* [ALK5], and *ACVR1C* [ALK7]), and DAPT (*NOTCH1-4* and its ligands *DLL1,3,4* and *JAG1,2*). Levels are shown relative to those observed across all 25 tissues shown in Figure 3A.

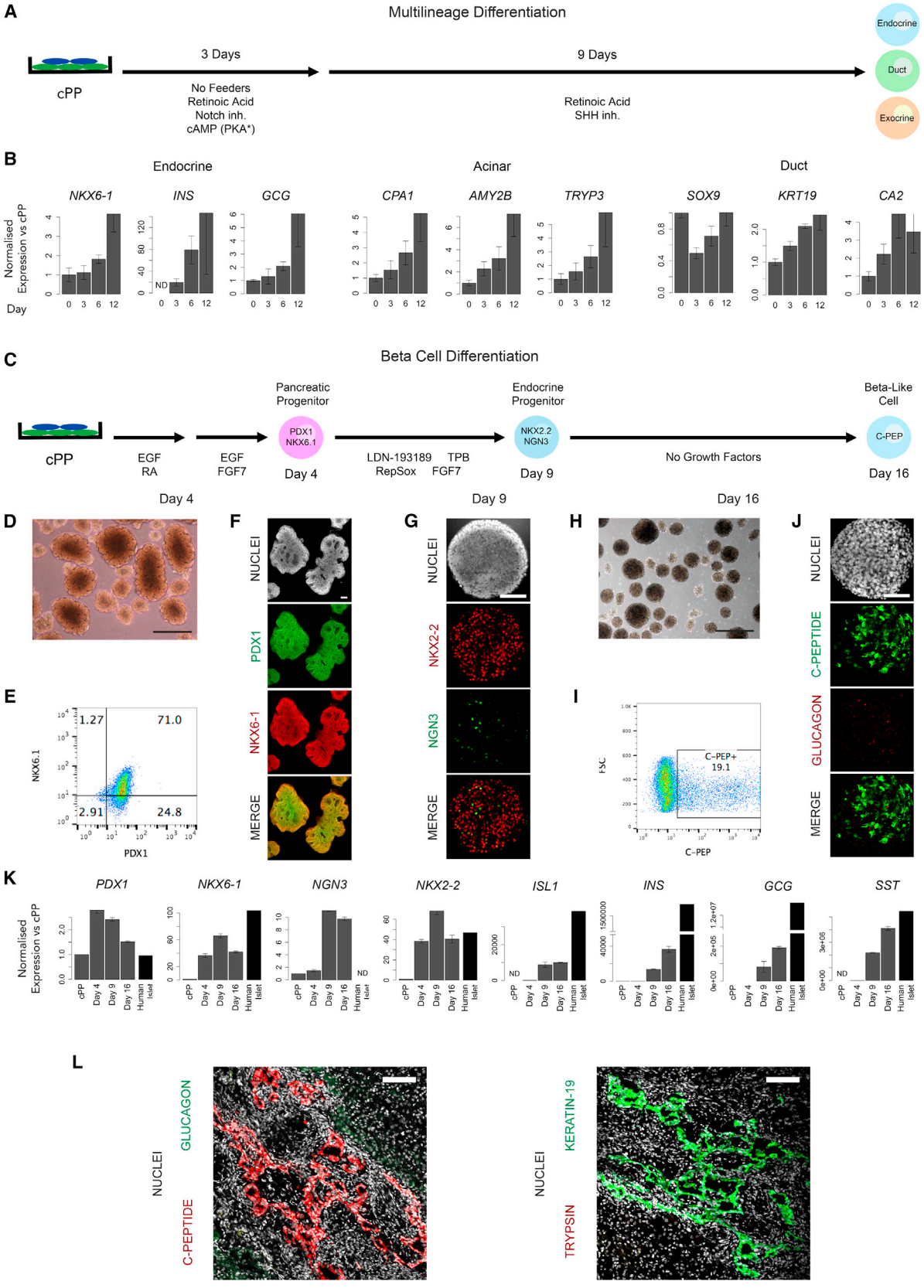

(legend on next page)

in vivo. Accordingly, none of the 12 mice we assessed exhibited teratoma formation, despite transplanting >3 million cells into each mouse. These observations demonstrate that cPP cells retain the ability to differentiate into endocrine and duct cells in vivo, although it remains to be seen whether they are capable of forming acinar cells. Furthermore, the absence of teratoma formation suggests cPP cells may represent a safer alternative for transplantations than cells differentiated directly from pluripotent stem cells.

DISCUSSION

Pluripotent stem cells have been proposed as an unlimited source of β cells for modeling and treating diabetes. However, the routine generation of functional β cells from diverse patient-derived hiPSC remains a challenge, partly because of the variability inherent in long, multi-step-directed differentiation protocols. Here, we describe a platform for long-term culture of self-renewing pancreatic progenitor cells derived from human pluripotent stem cells. These cPP cells are capable of rapid and prolonged expansion, thereby offering a convenient alternative source of β cells. Furthermore, cPP cells can be stored and transported as frozen stocks, and to date we have cultured cPP cells for up to 25 passages with no loss of proliferation. We observed that cPP cells express markers of pancreatic endocrine, duct, and acinar cells when differentiated in vitro, thereby demonstrating their multipotency, and we were able to generate up to ~20% C-peptide+ cells using a modified version of the β cell differentiation protocol described by Russ et al. (2015). The definitive test of developmental potency is whether a cell can differentiate into a particular lineage in vivo, and cPP cells indeed generate significant numbers of keratin-19+ duct cells and C-peptide+ β-like cells when transplanted under the renal capsule of an immunodeficient mouse, although it is unclear whether they retain the ability to form acinar cells in vivo.

Cells differentiating in vitro typically do so in an unsynchronized manner, causing cultures to become progressively more heterochronic with time and reducing the efficiency with which cells can be directed toward particular lineages. Therefore, the ability to capture and synchronize differentiating progenitors is essential for developing robust protocols for generating functional β cells from diverse genetic backgrounds. Extensive molecular characterization revealed that cPP cultures generated from both hESC and hiPSC represent stable populations of cells that express early pancreatic transcription factors consistently over time. The cPP transcriptome is closely related to that of the progenitor cells of the CS16-18 pancreas. However, comparison with human embryos at different stages of development suggests that cPP cells most closely resemble cells of the pancreatic bud between CS12 and CS13, based on robust expression of PDX1, SOX9, FOXA2, and GATA4/6 and the absence of NKX6-1 and SOX17 (Jennings et al., 2013, 2015).

In recent years, several groups reported methods for culturing human endodermal derivatives. Two separate reports demonstrated that hESC-derived definitive endoderm can be serially passaged and expanded if cultured on a feeder layer in the presence of appropriate mitogenic signals (Cheng et al., 2012; Sneddon et al., 2012). Subsequently, another group showed that foregut progenitor cells can be cultured in feeder-free conditions (Hannan et al., 2013). However, slow growth and variable gene expression between different lines have limited their utility. More recently, it was shown that pancreatic progenitors derived from reprogrammed endodermal cells could

Figure 5. Testing cPP Potency In Vitro and In Vivo

(A) Feeder-depleted passage 15 H9 cPP cells were replated on Matrigel and exposed to the indicated factors that promote multilineage differentiation toward the endocrine, duct, and acinar lineages.

(B) Endocrine, exocrine, and ductal gene expression analysis in (A) after 3, 6, and 12 days. Values are shown relative to levels in undifferentiated cPP cells (day 0). Error bars represent the SE of three technical replicates.

(C) Directed differentiation of passage 10 AK6-13 cPP cells to insulin+ β-like cells using a modified version of Russ et al. (2015).

(D) Phase-contrast image of differentiating spheres undergoing branching morphogenesis after 4 days. Scale bar, 100 μm.

(E) Intracellular flow cytometric analysis of day 4 cells shows approximately 70% reactivate NKX6-1 and maintain PDX1.

(F) PDX1 and NKX6-1 immunostaining on day 4. Scale bar, 100 μm.

(G) On day 9, the majority of cells are NKX2-2+ with a proportion of these transiently NGN3+. Scale bar, 100 μm.

(H) Phase contrast image of day 16 spheres. Scale bar, 100 μm.

(I) Approximately 20% of cells are C-peptide+ on day 16.

(J) Day 16 C-peptide+ cells do not coexpress glucagon. Scale bar, 100 μm.

(K) Gene expression measured by qRT-PCR of cPP cells on days 4, 9, and 16 harvested from the differentiation protocol in (C). Levels are shown relative to those in undifferentiated cPP cells and human islets for comparison. Error bars represent the SE of three technical replicates.

(L) Immunostaining of transplanted cPP cells for markers of endocrine (C-peptide and glucagon), duct (keratin-19), and acinar (trypsin) lineages. Scale bar, 100 μm.

be expanded and passaged (Zhu et al., 2015). However, these cultures are highly heterogeneous, and it is not clear whether the minimal combination of signaling molecules and inhibitors used is sufficient to culture cells from different genetic backgrounds. Therefore, the culture system described here is the first to enable long-term self-renewal of multipotent pancreatic progenitors derived from genetically diverse hESC and hiPSC.

Intriguingly, 3T3-J2 feeders have been used to culture diverse cells types, including epidermal keratinocytes (Rheinwald and Green, 1975a, 1975b), corneal epithelium (Osei-Bempong et al., 2009; Rama et al., 2010), and intestinal stem cells (Wang et al., 2015), among others. Nonetheless, the mechanism(s) by which 3T3-J2 feeders stabilize cultured progenitors are unknown. An obvious candidate is signaling through the WNT/LGR5 pathway, which is required for the maintenance of organoid cultures generated from a variety of endoderm-derived adult tissues, including the pancreas (Barker et al., 2007, 2010; Boj et al., 2015; Huch et al., 2013). However, cPP cells do not express LGR5 and are unaffected by inhibition of endogenous WNT secretion (data not shown). Therefore, identification of the factor(s) produced by 3T3-J2 cells could lead to the discovery of a common signaling axis required to support self-renewal of progenitors from a wide variety of tissues. Finally, it will be interesting to investigate whether adapted versions of the culture system described here are capable of capturing progenitors from other endoderm-derived tissues, such as the liver, stomach, and lung, or progenitors resident in the adult pancreas.

EXPERIMENTAL PROCEDURES

Human Pluripotent Stem Cell Culture and Differentiation

Human pluripotent cell lines were obtained as described in the Supplemental Experimental Procedures. Pluripotent stem cells were maintained on tissue culture plastic coated with Matrigel in mTeSR1 medium as described previously (Ludwig et al., 2006), and differentiated into pancreatic progenitors using the STEMdiff Pancreatic Progenitor kit (STEMCELL Technologies, 05120) according to the manufacturer's instructions with the following modifications: (1) cells were initially seeded into 12-well plates (Corning, 353043) at a density of 10^6 cells/well, and (2) stage 1 was extended to 3 days by repeating the final day's treatment. All tissue culture was carried out in 5% CO_2 at 37°C.

Passaging and Maintenance of cPP Cells

Gentle cell dissociation reagent (STEMCELL Technologies, 07174) was used to passage cPP cells as aggregates that were then seeded at a 1:6 split ratio onto a layer of 3T3-J2 feeders (0.5×10^6 to 1×10^6 cells/cm^2) in medium composed of advanced DMEM/F12 (Thermo Fisher Scientific, 21634010), 2 mM L-glutamine (Thermo Fisher Scientific, 25030), 100 U/mL penicillin/streptomycin (Thermo Fisher Scientific, 15140122), 1× N2 supplement (Thermo Fisher Scientific, 17502-048), 1× B27 supplement (Thermo Fisher Scientific, 17504-044), 30 nM dexamethasone (STEMCELL Technologies, 72092), 50 ng/mL EGF (R&D Systems, 236-EG-200), 50 ng/mL FGF10 (Source Bioscience, ABC144), 3 μM RA (Sigma, R2625), 10 μM SB431542 (Calbiochem, 616464), and 1 μM DAPT (Sigma, D5942). If plating single cPP cells, complete medium was supplemented with 10 μM Y27632 for the first 48 hr (Sigma, Y0503). Medium was completely replenished every 2–3 days. See Supplemental Experimental Procedures for details of 3T3-J2 cell culture.

RNA-Seq Analysis of Gene Expression

RNA was isolated from samples harvested from cPP and PPd15 cultures using an RNeasy mini kit (QIAGEN, cat. no. 74104). Feeder removal microbeads (Miltenyi Biotec, 130-095-531) were used to deplete cPP cells of 3T3 feeders prior to RNA extraction. All RNA samples had an RNA integrity number >9. RNA-seq libraries were generated using the NEBNext Ultra RNA Library Prep Kit (NEB, E7530L) and sequenced on an Illumina HiSeq 2500 system generating single-end reads of 100 bp. Table S1 contains metadata for these and public datasets used for the RNA-seq gene expression analysis. Full details of how RNA-seq reads were aligned and analyzed can be found in the Supplemental Experimental Procedures.

Multilineage Differentiation

Monolayer differentiation cultures were established as described in Supplemental Experimental Procedures. Basal differentiation medium consists of advanced DMEM/F12 (Thermo Fisher Scientific, 21634010), 2.5 g/30 mL BSA (Sigma, A9418), 2 mM L-glutamine (Thermo Fisher Scientific, 25030), 100 U/mL penicillin/streptomycin (Thermo Fisher Scientific, 15140122), and 1× B27 supplement (Thermo Fisher Scientific, 17504-044). Supplements were added as follows: days 1–3 (3 μM RA [Sigma, R2625], 1 μM DAPT [Sigma, D5942], 100 μM BNZ [Sigma, B4560]) and days 4, 7, and 10 (3 μM RA, 167 ng/mL KAAD-cyclopamine [Calbiochem, 239807]).

β Cell Differentiation

Differentiation sphere cultures were established as described in Supplemental Experimental Procedures. Basal differentiation medium consists of DMEM high glucose, 2 mM L-glutamine, and 100 U/mL penicillin/streptomycin. Supplements were added as follows: days 1–4 (1× B27 supplement, 50 ng/mL EGF, 1 μM RA [days 1–2 only], 50 ng/mL FGF7 [days 3–4 only]); days 5–10 (1× B27 supplement, 500 nM LDN-193189 [STEMCELL Technologies, 72142], 30 nM TPB [EMD Millipore, 565740], 1 μM RepSox [STEMCELL Technologies, 72392], 25 ng/mL FGF7); and days 11-17 (DMEM low glucose [Thermo Fisher Scientific, 12320-032], 2 mM L-glutamine, 1× MEM non-essential amino acids [Thermo Fisher Scientific, 11140-050]).

Transplantation Assays

cPP cells were grown to confluency to displace and eliminate feeder cells, then treated with gentle cell dissociation reagent to generate single cells. Approximately 3×10^6 to 5×10^6 cells were

resuspended in 50 μL of undiluted Matrigel and injected under the kidney capsule of 8- to 12-week-old immunocompromised (NOD/SCID) mice. After 23–27 weeks, transplanted mice were euthanized and their kidneys cryopreserved prior to sectioning and immunostaining. The study protocol was approved by the National University of Singapore Institutional Review Board (NUS IRB 12–181) and Biomedical Research Council IACUC committee (151040).

ACCESSION NUMBERS

Primary RNA-seq datasets generated here are available at ArrayExpress under accession number ArrayExpress: E-MTAB-5731.

SUPPLEMENTAL INFORMATION

Supplemental Information includes Supplemental Experimental Procedures, five figures, and three tables and can be found with this article online at http://dx.doi.org/10.1016/j.stemcr.2017.05.019.

AUTHOR CONTRIBUTIONS

Conceptualization and Methodology, J.T. and N.R.D.; Investigation, J.T., E.K.T., S.O., J.W., D.M.T., and M.L.; Formal Analysis, J.T., S.L.I.J.D., M.L., and D.M.T.; Resources, M.S., J.C.W., and B.R.; Writing – Original Draft, J.T. and N.R.D.; Funding Acquisition, N.R.D., J.C.W., L.S., G.R., B.R., and S.C.

ACKNOWLEDGMENTS

We thank Dr. Aya Wada and Prof. Huck Hui Ng for advice and guidance on cell culture techniques. We would also like to thank Dr. Michael Riedel, Dr. Jenna Moccia, and Dr. Charis Segeritz-Walko of STEMCELL Technologies for providing differentiation reagents, and Dr. Kim Robinson, Prof. Birgit Lane, and Prof. Yann Barrandon for supplying 3T3-J2 feeder cells. This work was funded by an EDB Singapore Childhood Undiagnosed Diseases Program grant and an A*STAR Strategic Positioning Fund (SPF) Genetic Orphan Diseases Adopted: Fostering Innovation Therapy (GODAFIT) grant.

Received: March 14, 2017
Revised: May 15, 2017
Accepted: May 15, 2017
Published: June 6, 2017

REFERENCES

Barker, N., van Es, J.H., Kuipers, J., Kujala, P., van den Born, M., Cozijnsen, M., Haegebarth, A., Korving, J., Begthel, H., Peters, P.J., and Clevers, H. (2007). Identification of stem cells in small intestine and colon by marker gene Lgr5. Nature *449*, 1003–1007.

Barker, N., Huch, M., Kujala, P., van de Wetering, M., Snippert, H.J., van Es, J.H., Sato, T., Stange, D.E., Begthel, H., van den Born, M., et al. (2010). LGR5+ve stem cells drive self-renewal in the stomach and build long-lived gastric units in vitro. Cell Stem Cell *6*, 25–36.

Bernstein, B.E., Stamatoyannopoulos, J.A., Costello, J.F., Ren, B., Milosavljevic, A., Meissner, A., Kellis, M., Marra, M.A., Beaudet, A.L., Ecker, J.R., et al. (2010). The NIH roadmap epigenomics mapping consortium. Nat. Biotechnol. *28*, 1045–1048.

Bhushan, A., Itoh, N., Kato, S., Thiery, J.P., Czernichow, P., Bellusci, S., and Scharfmann, R. (2001). Fgf10 is essential for maintaining the proliferative capacity of epithelial progenitor cells during early pancreatic organogenesis. Development *128*, 5109–5117.

Boj, S.F., Hwang, C.I., Baker, L.A., Chio, I.I.C., Engle, D.D., Corbo, V., Jager, M., Ponz-Sarvise, M., Tiriac, H., Spector, M.S., et al. (2015). Organoid models of human and mouse ductal pancreatic cancer. Cell *160*, 324–338.

Cahan, P., and Daley, G.Q. (2013). Origins and implications of pluripotent stem cell variability and heterogeneity. Nat. Rev. Mol. Cell Biol. *14*, 357–368.

Cebola, I., Rodríguez-Seguí, S.A., Cho, C.H.H., Bessa, J., Rovira, M., Luengo, M., Chhatriwala, M., Berry, A., Ponsa-Cobas, J., Maestro, M.A., et al. (2015). TEAD and YAP regulate the enhancer network of human embryonic pancreatic progenitors. Nat. Cell Biol. *17*, 615–626.

Cheng, X., Ying, L., Lu, L., Galvão, A.M., Mills, J.A., Lin, H.C., Kotton, D.N., Shen, S.S., Nostro, M.C., Choi, J.K., et al. (2012). Self-renewing endodermal progenitor lines generated from human pluripotent stem cells. Cell Stem Cell *10*, 371–384.

Conrad, E., Stein, R., and Hunter, C.S. (2014). Revealing transcription factors during human pancreatic β cell development. Trends Endocrinol. Metab. *25*, 407–414.

Hald, J., Hjorth, J.P., German, M.S., Madsen, O.D., Serup, P., and Jensen, J. (2003). Activated Notch1 prevents differentiation of pancreatic acinar cells and attenuate endocrine development. Dev. Biol. *260*, 426–437.

Hannan, N.R.F., Fordham, R.P., Syed, Y.A., Moignard, V., Berry, A., Bautista, R., Hanley, N.A., Jensen, K.B., and Vallier, L. (2013). Generation of multipotent foregut stem cells from human pluripotent stem cells. Stem Cell Reports *1*, 293–306.

Hart, A., Papadopoulou, S., and Edlund, H. (2003). Fgf10 maintains notch activation, stimulates proliferation, and blocks differentiation of pancreatic epithelial cells. Dev. Dyn. *228*, 185–193.

Huch, M., Bonfanti, P., Boj, S.F., Sato, T., Loomans, C.J.M., van de Wetering, M., Sojoodi, M., Li, V.S.W., Schuijers, J., Gracanin, A., et al. (2013). Unlimited in vitro expansion of adult bi-potent pancreas progenitors through the Lgr5/R-spondin axis. EMBO J. *32*, 2708–2721.

Jennings, R.E., Berry, A.A., Kirkwood-Wilson, R., Roberts, N.A., Hearn, T., Salisbury, R.J., Blaylock, J., Piper Hanley, K., and Hanley, N.A. (2013). Development of the human pancreas from foregut to endocrine commitment. Diabetes *62*, 3514–3522.

Jennings, R.E., Berry, A.A., Strutt, J.P., Gerrard, D.T., and Hanley, N.A. (2015). Human pancreas development. Development *142*, 3126–3137.

Jonsson, J., Carlsson, L., Edlund, T., and Edlund, H. (1994). Insulin-promoter-factor 1 is required for pancreas development in mice. Nature *371*, 606–609.

Kroon, E., Martinson, L.A., Kadoya, K., Bang, A.G., Kelly, O.G., Eliazer, S., Young, H., Richardson, M., Smart, N.G., Cunningham, J., et al. (2008). Pancreatic endoderm derived from human embryonic stem cells generates glucose-responsive insulin-secreting cells in vivo. Nat. Biotechnol. *26*, 443–452.

Ludwig, T.E., Bergendahl, V., Levenstein, M.E., Yu, J., Probasco, M.D., and Thomson, J.A. (2006). Feeder-independent culture of human embryonic stem cells. Nat. Methods *3*, 637–646.

Martín, M., Gallego-Llamas, J., Ribes, V., Kedinger, M., Niederreither, K., Chambon, P., Dollé, P., and Gradwohl, G. (2005). Dorsal pancreas agenesis in retinoic acid-deficient Raldh2 mutant mice. Dev. Biol. *284*, 399–411.

McCracken, K.W., Catá, E.M., Crawford, C.M., Sinagoga, K.L., Schumacher, M., Rockich, B.E., Tsai, Y.-H., Mayhew, C.N., Spence, J.R., Zavros, Y., and Wells, J.M. (2014). Modelling human development and disease in pluripotent stem-cell-derived gastric organoids. Nature *516*, 400–404.

Miettinen, P.J., Huotari, M., Koivisto, T., Ustinov, J., Palgi, J., Rasilainen, S., Lehtonen, E., Keski-Oja, J., and Otonkoski, T. (2000). Impaired migration and delayed differentiation of pancreatic islet cells in mice lacking EGF-receptors. Development *127*, 2617–2627.

Murtaugh, L.C., Stanger, B.Z., Kwan, K.M., and Melton, D.A. (2003). Notch signaling controls multiple steps of pancreatic differentiation. Proc. Natl. Acad. Sci. USA *100*, 14920–14925.

Nostro, M.C., Sarangi, F., Yang, C., Holland, A., Elefanty, A.G., Stanley, E.G., Greiner, D.L., and Keller, G. (2015). Efficient generation of NKX6-1+ pancreatic progenitors from multiple human pluripotent stem cell lines. Stem Cell Reports *4*, 591–604.

Offield, M.F., Jetton, T.L., Labosky, P.A., Ray, M., Stein, R.W., Magnuson, M.A., Hogan, B.L., and Wright, C.V. (1996). PDX-1 is required for pancreatic outgrowth and differentiation of the rostral duodenum. Development *122*, 983–995.

Osei-Bempong, C., Henein, C., and Ahmad, S. (2009). Culture conditions for primary human limbal epithelial cells. Regen. Med. *4*, 461–470.

Pagliuca, F.W., Millman, J.R., Gürtler, M., Segel, M., Van Dervort, A., Ryu, J.H., Peterson, Q.P., Greiner, D., and Melton, D.A. (2014). Generation of functional human pancreatic β cells in vitro. Cell *159*, 428–439.

Pan, F.C., and Wright, C. (2011). Pancreas organogenesis: from bud to plexus to gland. Dev. Dyn. *240*, 530–565.

Petryszak, R., Burdett, T., Fiorelli, B., Fonseca, N.A., Gonzalez-Porta, M., Hastings, E., Huber, W., Jupp, S., Keays, M., Kryvych, N., et al. (2013). Expression Atlas update—a database of gene and transcript expression from microarray- and sequencing-based functional genomics experiments. Nucleic Acids Res. *42*, D926–D932.

Rama, P., Matuska, S., Paganoni, G., Spinelli, A., De Luca, M., and Pellegrini, G. (2010). Limbal stem-cell therapy and long-term corneal regeneration. N. Engl. J. Med. *363*, 147–155.

Rezania, A., Bruin, J.E., Arora, P., Rubin, A., Batushansky, I., Asadi, A., O'Dwyer, S., Quiskamp, N., Mojibian, M., Albrecht, T., et al. (2014). Reversal of diabetes with insulin-producing cells derived in vitro from human pluripotent stem cells. Nat. Biotechnol. *32*, 1121–1133.

Rheinwald, J.G., and Green, H. (1975a). Formation of a keratinizing epithelium in culture by a cloned cell line derived from a teratoma. Cell *6*, 317–330.

Rheinwald, J.G., and Green, H. (1975b). Serial cultivation of strains of human epidermal keratinocytes: the formation of keratinizing colonies from single cells. Cell *6*, 331–343.

Rostovskaya, M., Bredenkamp, N., and Smith, A. (2015). Towards consistent generation of pancreatic lineage progenitors from human pluripotent stem cells. Philos. Trans. R. Soc. Lond. B Biol. Sci. *370*, 20140365.

Russ, H.A., Parent, A.V., Ringler, J.J., Hennings, T.G., Nair, G.G., Shveygert, M., Guo, T., Puri, S., Haataja, L., Cirulli, V., et al. (2015). Controlled induction of human pancreatic progenitors produces functional beta-like cells in vitro. EMBO J. *34*, 1759–1772.

Schwitzgebel, V.M., Scheel, D.W., Conners, J.R., Kalamaras, J., Lee, J.E., Anderson, D.J., Sussel, L., Johnson, J.D., and German, M.S. (2000). Expression of neurogenin3 reveals an islet cell precursor population in the pancreas. Development *127*, 3533–3542.

Shih, H.P., Wang, A., and Sander, M. (2013). Pancreas organogenesis: from lineage determination to morphogenesis. Annu. Rev. Cell Dev. Biol. *29*, 81–105.

Shih, H.P., Seymour, P.A., Patel, N.A., Xie, R., Wang, A., Liu, P.P., Yeo, G.W., Magnuson, M.A., and Sander, M. (2015). A gene regulatory network cooperatively controlled by Pdx1 and Sox9 governs lineage allocation of foregut progenitor cells. Cell Rep. *13*, 326–336.

Sneddon, J.B., Borowiak, M., and Melton, D.A. (2012). Self-renewal of embryonic-stem-cell-derived progenitors by organ-matched mesenchyme. Nature *491*, 765–768.

Titmarsh, D.M., Hudson, J.E., Hidalgo, A., Elefanty, A.G., Stanley, E.G., Wolvetang, E.J., and Cooper-White, J.J. (2012). Microbioreactor arrays for full factorial screening of exogenous and paracrine factors in human embryonic stem cell differentiation. PLoS One *7*, e52405.

Wang, X., Yamamoto, Y., Wilson, L.H., Zhang, T., Howitt, B.E., Farrow, M.A., Kern, F., Ning, G., Hong, Y., Khor, C.C., et al. (2015). Cloning and variation of ground state intestinal stem cells. Nature *522*, 173–178.

Ye, F., Duvilli, B., and Scharfmann, R. (2005). Fibroblast growth factors 7 and 10 are expressed in the human embryonic pancreatic mesenchyme and promote the proliferation of embryonic pancreatic epithelial cells. Diabetologia *48*, 277–281.

Zhang, D., Jiang, W., Liu, M., Sui, X., Yin, X., Chen, S., Shi, Y., and Deng, H. (2009). Highly efficient differentiation of human ES cells and iPS cells into mature pancreatic insulin-producing cells. Cell Res. *19*, 429–438.

Zhu, S., Russ, H.A., Wang, X., Zhang, M., Ma, T., Xu, T., Tang, S., Hebrok, M., and Ding, S. (2015). Human pancreatic beta-like cells converted from fibroblasts. Nat. Commun. *7*, 1–13.

Stem Cell Reports, Volume *8*

Supplemental Information

Long-Term Culture of Self-renewing Pancreatic Progenitors Derived from Human Pluripotent Stem Cells

Jamie Trott, Ee Kim Tan, Sheena Ong, Drew M. Titmarsh, Simon L.I.J. Denil, Maybelline Giam, Cheng Kit Wong, Jiaxu Wang, Mohammad Shboul, Michelle Eio, Justin Cooper-White, Simon M. Cool, Giulia Rancati, Lawrence W. Stanton, Bruno Reversade, and N. Ray Dunn

A

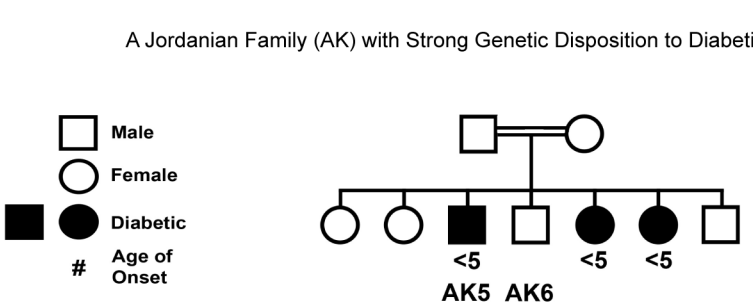
A Jordanian Family (AK) with Strong Genetic Disposition to Diabetic Beta Cell Failure
Male
Female
Diabetic
Age of Onset
<5
<5
<5
AK5
AK6

B


AK5 Clone 11 (AK5-11)
AK6 Clone 13 (AK6-13)
OCT4+
92.5
OCT4+
96.6
Count
OCT4

C

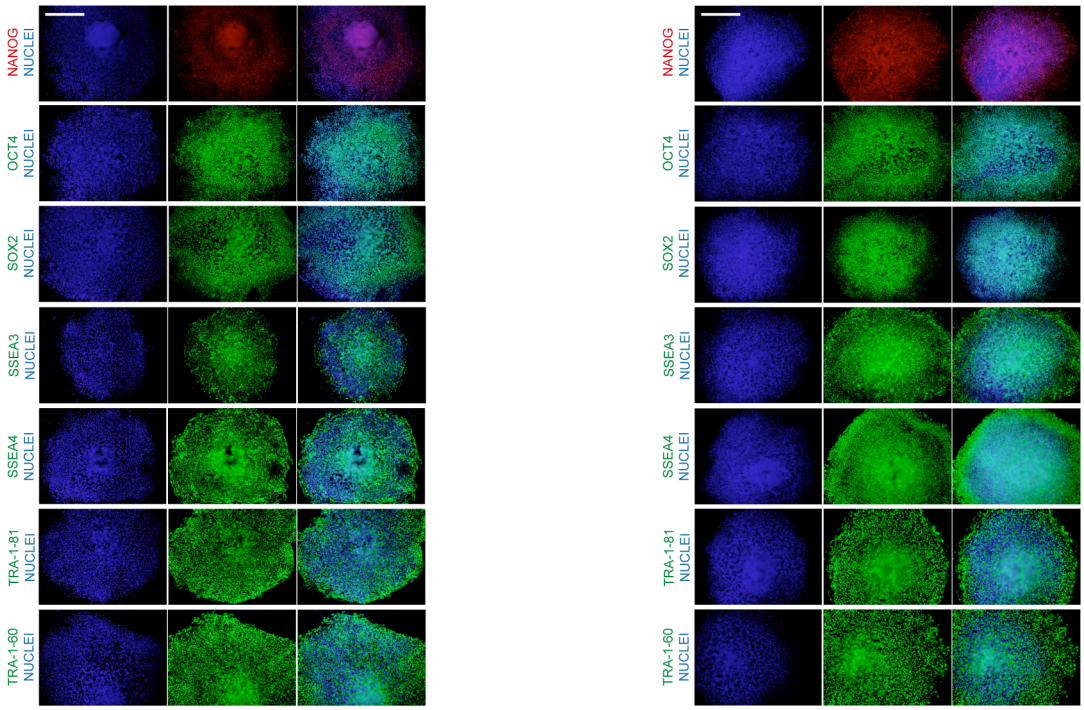
NANOG NUCLEI
OCT4 NUCLEI
SOX2 NUCLEI
SSEA3 NUCLEI
SSEA4 NUCLEI
TRA-1-81 NUCLEI
TRA-1-60 NUCLEI

Figure S1: Generation of hiPSC lines from diabetic and healthy sibling fibroblasts.

A) Pedigree of a consanguineous Jordanian family with several diabetic siblings. All diabetic siblings developed the disease before 5 years of age. Skin biopsies taken from individuals AK5 and AK6 were used to generate fibroblasts from which hiPSC were derived.

B) Intracellular flow cytometric analysis of OCT4 expression and C) Immunostaining for established markers of pluripotency for hiPSC clones AK5-11, AK6-13 and AK6-8 (not shown). Scale bar, 100 μm.

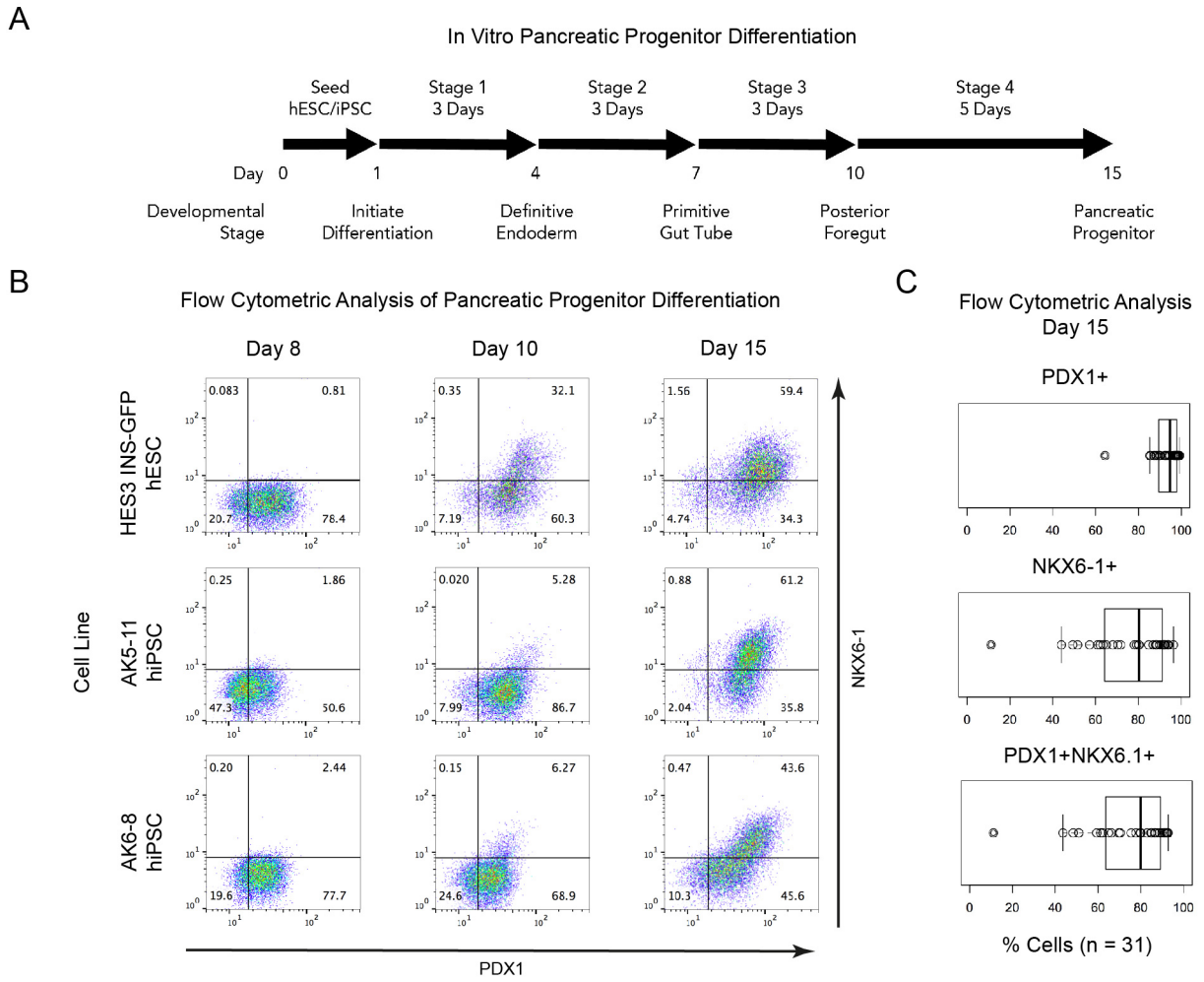
A
In Vitro Pancreatic Progenitor Differentiation
Seed hESC/iPSC
Stage 1 3 Days
Stage 2 3 Days
Stage 3 3 Days
Stage 4 5 Days
Day 0 1 4 7 10 15
Developmental Stage
Initiate Differentiation
Definitive Endoderm
Primitive Gut Tube
Posterior Foregut
Pancreatic Progenitor
B
Flow Cytometric Analysis of Pancreatic Progenitor Differentiation
Day 8
Day 10
Day 15
HES3 INS-GFP hESC
AK5-11 hiPSC
AK6-8 hiPSC
Cell Line
NKX6-1
PDX1
C
Flow Cytometric Analysis Day 15
PDX1+
NKX6-1+
PDX1+NKX6.1+
% Cells (n = 31)
D
Established cPP Cell Lines Generated from Genetically Diverse iPSC and hESC (passage 6)
PDX1
FOXA2
GATA6
SOX9
HNF4A
RFX6
Log2 Normalised Expression
H9 #1
H9 #2
HES3
AK5-11 #1
AK5-11 #2
AK6-8
AK6-13

Figure S2: Directed differentiation of pancreatic progenitor cells and generation of cPP cells from diverse human pluripotent stem cell lines

A) Time-course of pancreatic progenitor differentiation protocol. In our experiments, stage 1 was extended to last 3 days, rather than 2 as per the manufacturer's instructions, by repeating the final day's treatment.

B) Intracellular flow cytometric analysis of PDX1 and NKX6-1 at days 8, 10 and 15 of differentiation using hES3 INS-GFP reporter hESC (Micallef et al., 2011; Titmarsh et al., 2016) and the in-house hiPSC lines AK5-11 and AK6-8. PDX1 is detected before NKX6-1 in all cases, although individual lines exhibit variable differentiation kinetics. Gates are based on cells stained with isotype control antibodies.

C) Percentage PDX1+ and/or NKX6-1+ at day 15 of differentiation. Each circle represents one of 31 independent experiments encompassing 2 hESC lines and 6 hiPSC lines. The vertical black bar shows the median percentage of cells that are PDX1+ (95%), NKX6-1+ (80%) or PDX1+NKX6-1+ (80%).

D) Gene expression measured by qRT-PCR using samples harvested from cPP cell lines at passage 6. We analyzed cPP cells derived from the following pluripotent cell lines: H9 and HES3 hESC, and AK5-11, AK6-8 and AK6-13 hiPSC. Two independent pedigrees were derived from H9 and AK5-11 cell lines. Expression levels are shown normalized to those of H9 hESC and are plotted on a $\log_2$ scale. Error bars represent the standard error of three technical replicates.

A

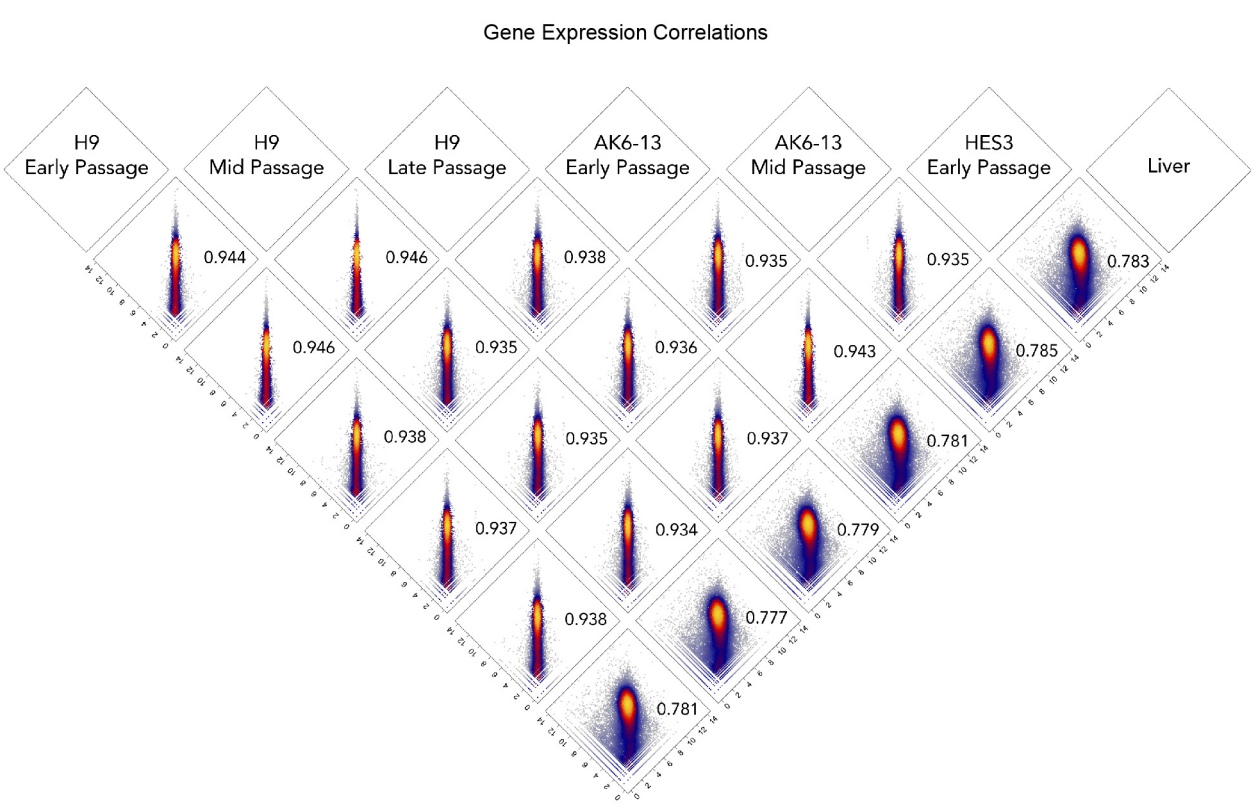
Gene Expression Correlations
H9 Early Passage
H9 Mid Passage
H9 Late Passage
AK6-13 Early Passage
AK6-13 Mid Passage
HES3 Early Passage
Liver
0.944
0.946
0.938
0.935
0.935
0.783
0.946
0.935
0.936
0.943
0.785
0.938
0.935
0.937
0.781
0.937
0.934
0.779
0.938
0.777
0.781

B

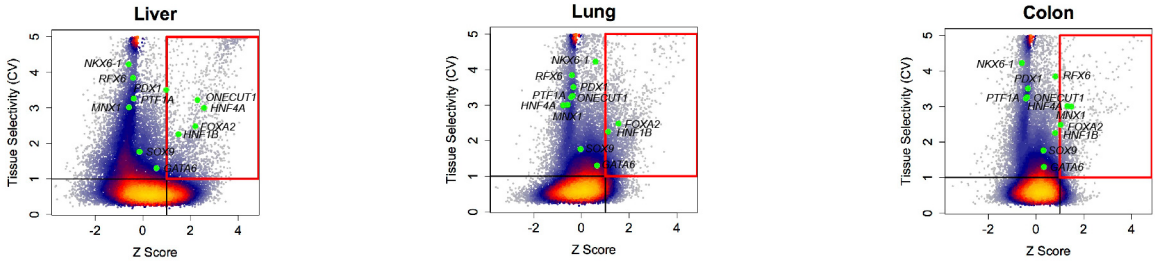
Specifically Expressed Genes
Liver
Lung
Colon
Tissue Selectivity (CV)
Z Score
NKX6-1
RFX6
PDX1
PTF1A
HNF4A
MNX1
ONECUT1
FOXA2
HNF1B
SOX9
GATA6

C

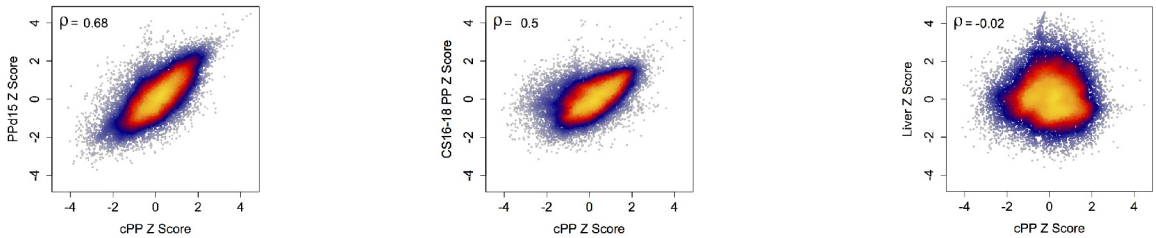
Z-Scores Correlations
ρ = 0.68
PPd15 Z Score
cPP Z Score
ρ = 0.5
CS16-18 PP Z Score
cPP Z Score
ρ = -0.02
Liver Z Score
cPP Z Score

Figure S3: Transcriptome analysis of cPP cells by RNA-seq.

A) Correlations between gene expression levels for cPP cells from three different genetic backgrounds (H9, AK6-13 and HES3) at early (6-8), mid (11-13) and late (18) passages. Log_2-transformed gene counts measured by RNA-seq were plotted for each gene. Gene counts in cPP samples are compared to liver for comparison. The Spearman correlation coefficient for each pair of samples is shown on the corresponding plot. Heat colors denote the number of transcripts. Gene counts are strongly correlated between cPP samples regardless of genetic background or passage number, but not with liver.

B) Identification of specifically expressed genes in liver, lung and colon samples. Genes associated with early pancreatic development are not typically found to be specifically expressed by these tissues.

C) Z-score correlations for cPP, PPd15, CS16-18 PP and liver samples. Z-scores are strongly correlated between in vitro and in vivo pancreatic progenitor samples but not between these samples and liver.

A

cPP Cells Plated in MBA Chamber

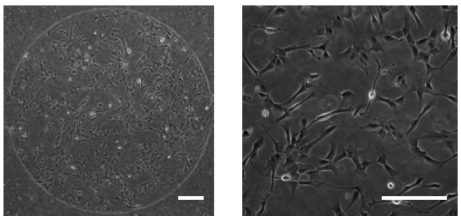

B

MBA Screening Protocol

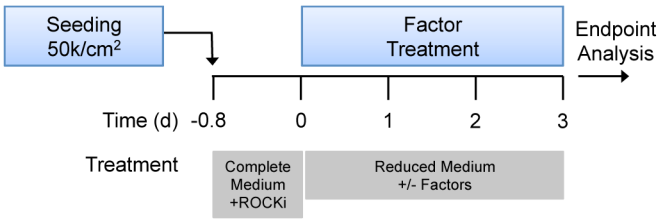

C

PDX1 SOX9

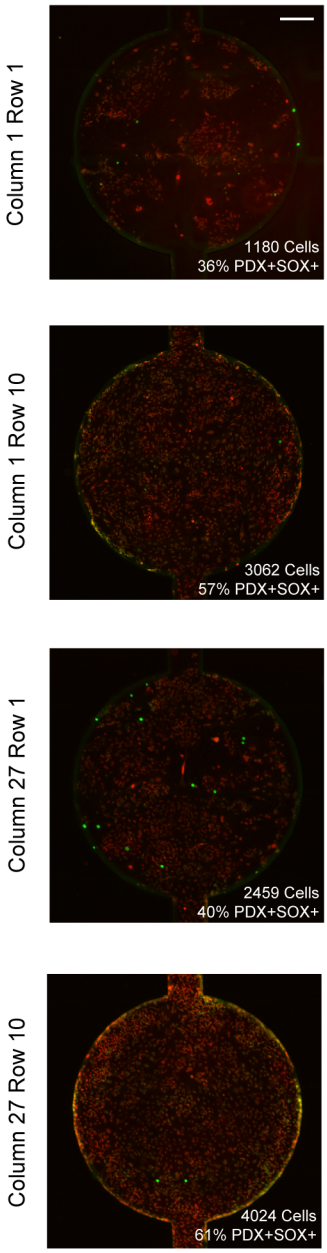

D

Processed Data Metrics for MBA Screen Extracted from Fluorescence Image

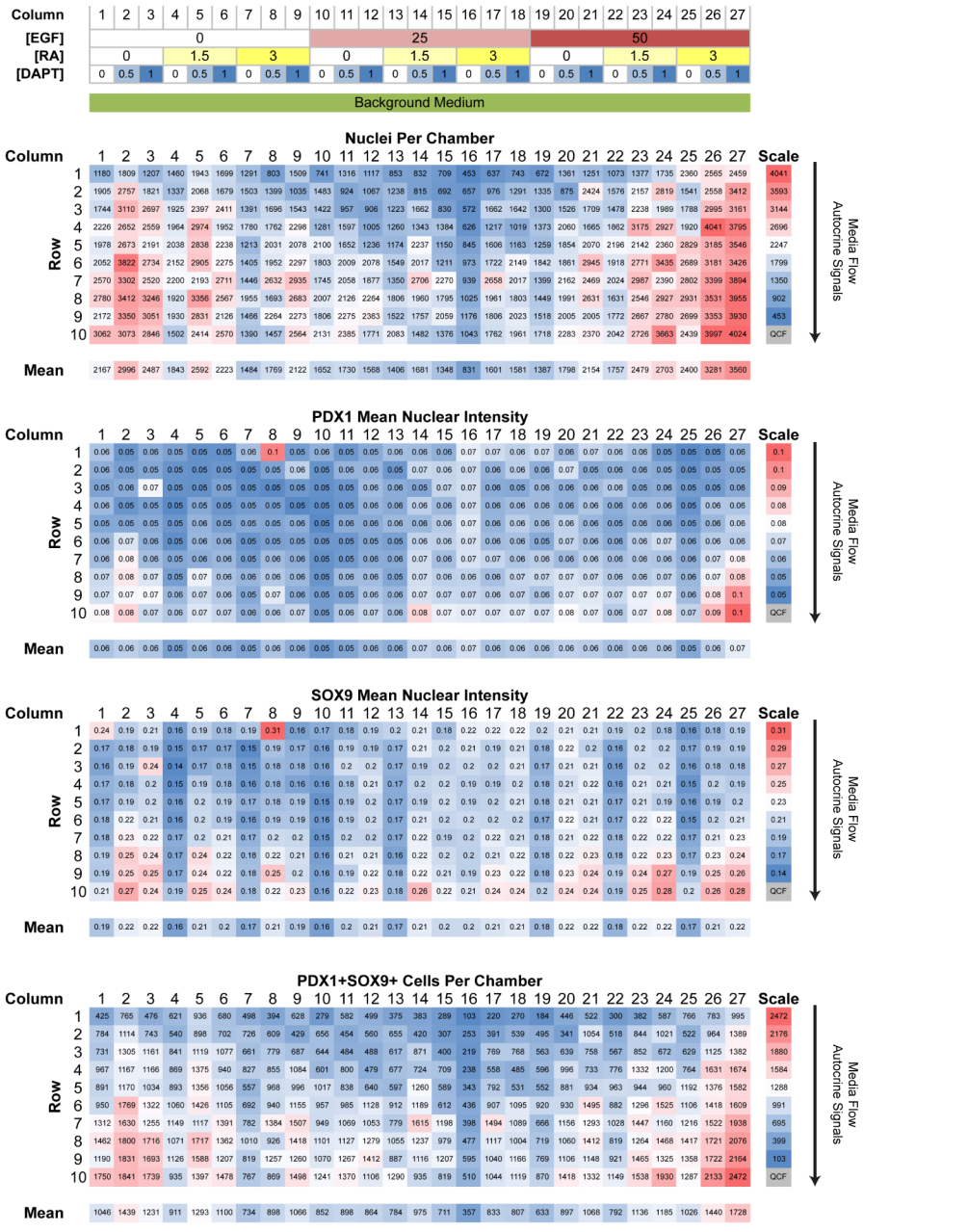

Figure S4: Microbioreactor Array (MBA) Screening of Factors Required to Propagate cPP Cells

A) Phase contrast images of $PDX1^{+}SOX9^{+}$ cPP cells seeded into Matrigel-coated MBAs and allowed to attach for 20 h with periodic feeding. Each MBA device has 270 chambers arranged as shown in S4D. Scale bar, 100 μm.

B) Protocol used for MBA screening.

C) Individual chambers of MBA device (270 culture chambers) stained with anti-PDX1 (green) and anti-SOX9 (red) antibodies. Hoechst 33342 (not shown) was used for nuclei identification. The chambers were selected to show the range of proliferation rates and protein expression observed across different signaling environments. Scale bar, 100 μm.

D) Endpoint measurements for each chamber in the MBA. Schematic above shows compositions of media applied to each column of the MBA (EGF, ng/mL; RA, μM; DAPT, μM). Cell culture media flow was from top (Row 1) to bottom (Row 10) down a column, thereby concentrating autocrine factors towards the bottom of the column. Mean measurements for each column are given below. QCF: data flagged for quality control issue during image processing. Values were extracted from images such as those in S4C using an image segmentation algorithm as described previously (Titmarsh et al., 2016).

Comparison of Published Beta Cell Differentiation Protocols - NKX6-1 Induction Step

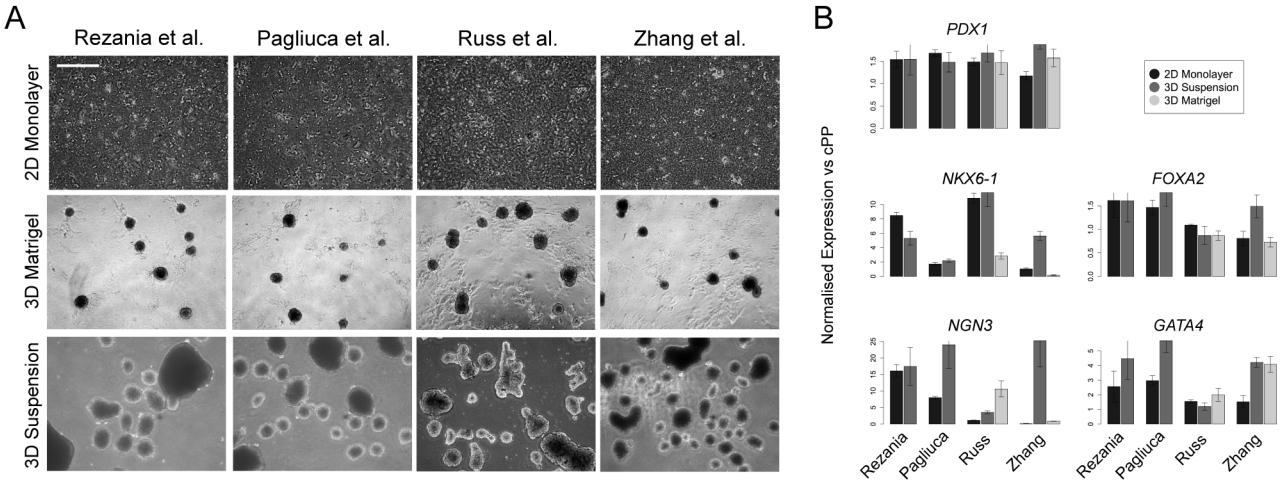

Optimization of NKX6-1 Induction Step of Russ et al. Beta Cell Differentiation Protocol

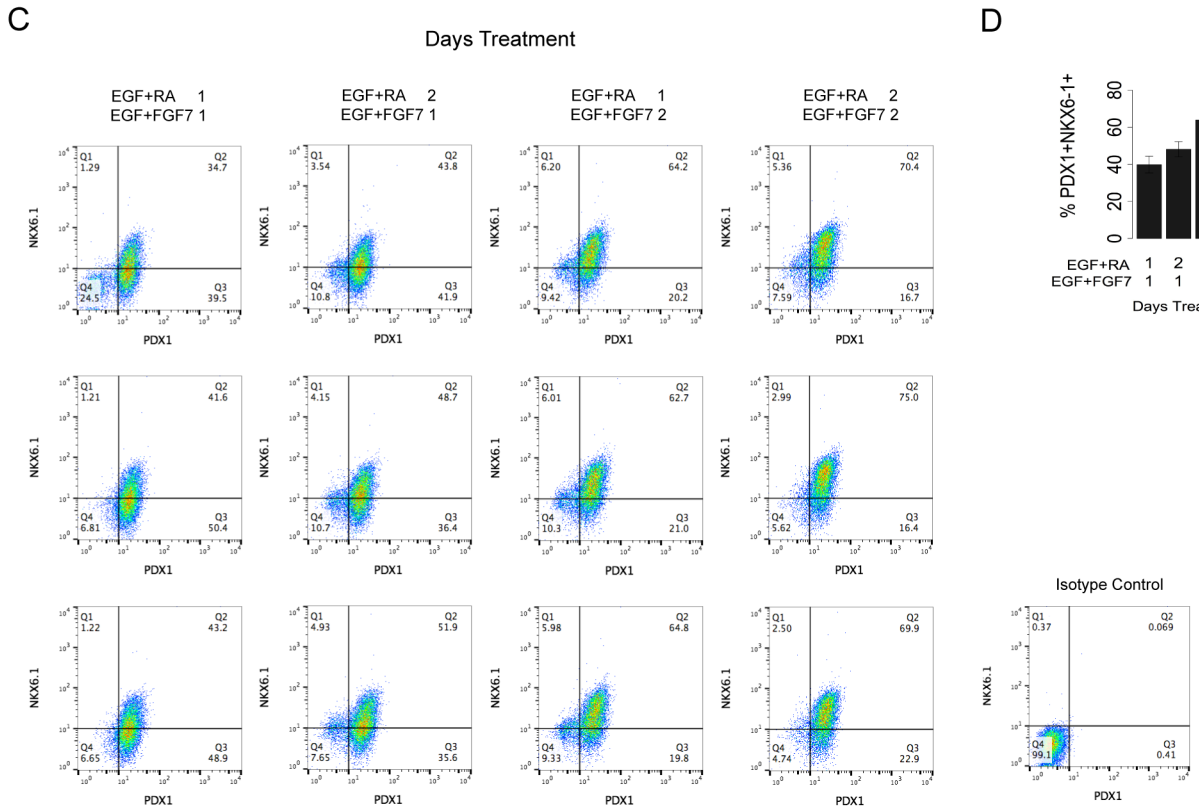

Figure S5: Optimization of cPP Beta Cell Differentiation

A) Application of NKX6-1 induction step of published beta cell differentiation protocols to cPP cells. We established 2D-monolayer, 3D-matrigel and 3D-suspension cultures in complete cPP media before exposing cells to growth factor regimes based on published beta cell differentiation protocols (see Supplementary Experimental Procedures). Phase contrast images were taken at the end of each treatment. Scale bar, 100 μm.

B) Gene expression measured by qRT-PCR using samples harvested in (A). When cells were exposed to the Rezania and Pagliuca differentiation regimes using the 3D matrigel platform, we were unable to recover sufficient material to carry out qRT-PCR analysis. Error bars represent the standard error of three technical replicates.

C) Optimization of the NKX6-1 induction step of the Russ et al. differentiation regime. Differentiations were carried out using the 3D-suspension platform. The lengths of the two growth factor treatments were varied to maximize the percentage of cells that reactivate NKX6-1 expression. PDX1 and NKX6-1 were measured by intracellular flow cytometric analysis. Three independent experiments are shown for each condition.

D) Percentage PDX1+NKX6-1+ cells generated in C.

Supplementary Table 1

Samples used for RNA-seq analysis.

Supplementary Table 2

Normalized gene counts for samples listed in supplementary table 1. The values for cPP and PPd15 cells are the mean values across the various samples listed in supplementary table 1. Genes (rows) are ordered according to the product of the coefficient of variance (column AI) and cPP Z-score (column AH). Raw RNA-seq read files are available for download at ArrayExpress under accession number E-MTAB-5731.

Supplementary Experimental Procedures

Human Pluripotent Stem Cell lines

The following hESC lines were used in this study: H9 (WA09) were purchased from WiCell, HES3 (ES03) were provided by ES Cell International Pte. Ltd., and the HES-3 *INS*$^{GFP/w}$ reporter line was a gift from the Stanley lab (Micallef et al., 2011). The hiPSC lines used in this study were derived in-house from human fibroblasts and are designated AK5-11, AK6-8 and AK6-13 (Figure S1).

Generation of hiPSC

Fibroblasts were obtained by punch skin biopsy and reprogrammed to generate hiPSC. Fibroblasts were reprogrammed using the CytoTune™-iPS 2.0 Sendai Reprogramming Kit (Thermo Fisher Scientific, A16517) in accordance with the manufacturer's instructions. Cells were passaged and plated onto irradiated mouse embryonic feeders 7 days after viral transfection. Thereafter, hiPSC colonies were picked between days 17-28 and maintained in DMEM/F12 (Sigma, D6421) supplemented with 20% Knock Out Serum Replacement (Thermo Fisher Scientific, 10828-028), 0.1 mM 2-mercaptoethanol (Thermo Fisher Scientific, 21985-023), 2 mM L-glutamine (Thermo Fisher Scientific, 25030), 0.2 mM NEAA (Thermo Fisher Scientific, 11140-050) and 5 ng/mL bFGF (Peprotech, 100-18B). Staining with the following antibodies was used to confirm pluripotency (Figure S1): NANOG (R&D Systems, AF1997, 1:200), OCT4 (Santa Cruz, 111351, 1:200), SOX2 (R&D Systems MAB2018, 1:200), SSEA3 (Millipore, MAB4303, 1:50), SSEA4 (Millipore, MAB4304, 1:200), TRA-1-81 (Millipore, MAB4381, 1:200), TRA-1-60 (Millipore, MAB4360, 1:200). Primary antibodies were recognized by Alexa-fluorophore conjugated secondary antibodies raised in Donkey (Thermo Fisher Scientific, 1:500). The study protocol was approved by the National University of Singapore Institutional Review Board (NUS IRB 10-051). The study was conducted in accordance with the Declaration of Helsinki and written informed consent was obtained from the participants.

Expansion of 3T3-J2 feeders

3T3-J2 feeder cells (passage 9, gift from Dr. Yann Barrandon) were expanded on tissue culture plastic (coated with 0.1% gelatin (Sigma, G2625) for 30 min) in 3T3-J2 culture media and passaged as single cells by treating with 0.25% Trypsin for 5 min (Thermo Fisher Scientific, 25200056). 3T3-J2 culture

media is composed of the following: DMEM high glucose (Thermo Fisher Scientific, 11960), 10% Fetal Bovine Serum (FBS, ES cell qualified, Thermo Fisher Scientific, 16141079), 2 mM L-glutamine (Thermo Fisher Scientific, 25030), and 100 U/mL penicillin/streptomycin (Thermo Fisher Scientific, 15140122). Feeder cells were mitotically inactivated by gamma irradiation (20 grays for 30 min) then frozen in culture media + DMSO. Individual batches of FBS are selected to enable 3T3-J2 cells to maintain cPP cultures, whilst 3T3-J2 cells are never cultured beyond passage 12 and should be seeded at 3.5-5x10^3 cells/cm^2 and not allowed to exceed 1.3x10^4 cells/cm^2.

Preparation of 3T3-J2 feeder-coated culture vessels

Thawed 3T3-J2 cells were seeded at 0.5-1x10^6 cells/cm^2 onto tissue culture plates coated with 0.1% gelatin (Sigma, G2625) for 30 min and maintained in 3T3-J2 culture media for up to 3 days until required. The optimal plating density must be determined empirically for each batch of feeders and is assessed based on the ability to maintain colony morphology without significantly hindering growth, since increasing feeder density improves colony morphology and blocks differentiation, but results in reduced proliferation rates. Tissue culture vessels containing feeders were washed once with DMEM to remove residual FBS prior to addition of cPP culture media.

Metaphase spread preparation, chromosome counting and M-FISH Karyotyping

Cells grown to ~75-80% confluency were treated with 100 ng/ml Colcemid solution (Gibco, 15212012) for 6 h, trypsinized and centrifuged at 1000 rpm for 10 min. Cell pellets were resuspended in 75 mM KCl and incubated for 15 min in a 37°C waterbath. 1/10 volume of 3:1 methanol/acetic acid was added to cells followed by centrifugation at 1000 rpm for 15 min. Cells were then fixed by resuspension in 3:1 methanol/acetic acid solution, incubated for 30 min at room temperature, centrifuged at 1200 rpm for 5 min and finally washed once more with fixative. Cells were resuspended in a small volume of fixative, dropped onto clean glass slides and left to air dry. Multicolor FISH (M-FISH) was performed according to manufacturer's instructions (MetaSystems). Automated acquisition of chromosome spreads was performed using Metafer imaging platform (MetaSystem). Ikaros and Fiji software were used to determine the chromosome number per spread and analyze M-FISH images.

RNA-seq read alignment, gene count calculation and normlization

Raw fastq files were downloaded with the fastq-dump function of the SRA-toolkit (v 2.8.0). We mapped reads with STAR (v2.5.1a) (Dobin et al., 2013) using an index based on the soft masked primary assembly of reference genome GRCh38 and corresponding gene annotation gtf file (GRCh38.83). Both were obtained from the Ensembl FTP site. Read overhang was set to 99 bp for index generation. Default mapping parameters were retained with the following exceptions: "--outFilterType BySJout" to reduce the number of spurious junctions, "--alignSJoverhangMin 10" minimum read overhang for unannotated junctions, "--alignSJDBoverhangMin 1" minimum overhang for annotated junctions, "--outFilterMatchNminOverLread 0.95" to allow up to 5% mismatched bases (per pair) if no better alignment can be found, "--alignIntronMin 20" to allow short introns, "--alignIntronMax 2000000" to set an upper limit on intron length, "--outMultimapperOrder Random" to randomize the choice of the primary alignment from the highest scoring alignments, "--outFilterIntronMotifs RemoveNoncanonicalUnannotated" to bias mapping towards known transcripts and "--chimSegmentMin 0" to suppress any chimeric mapping output.

The mapped reads of all samples were then jointly processed with featureCounts (Dobin et al., 2013; Liao et al., 2014) as implemented in the package "Rsubread" (v1.16.1) in R (v3.1.2). Default settings were used with the following exceptions: "annot.ext=GTFfile, isGTFAnnotationFile=TRUE, GTF.featureType='exon' " to use the same gtf annotation file as in STAR index, "useMetaFeatures=TRUE, GTF.attrType='gene' " to summarize counts to the gene level, "allowMultiOverlap=TRUE" to allow counting in overlapping genes, "isPairedEnd" was set as appropriate for the respective samples, "strandSpecific=0" because not all libraries were strand-specific and finally "countMultiMappingReads=TRUE". The resulting count table was normalized to account for sequencing depth and count distribution with the TMM method (Robinson and Oshlack, 2010) as implemented in edgeR (v3.8.6) using default settings.

Bioinformatics Analysis

RNA-seq gene expression analysis was carried out using normalized counts for each gene in each tissue type (Supplementary Table 2). Where technical replicates are available for samples described in other studies, we aligned these reads and determined gene counts separately, then calculated average

gene counts. Furthermore, unless otherwise stated, gene counts for cPP and PPd15 cells are the mean of three independent samples harvested from cells derived from H9 and HES3 hESC, and AK6-13 hiPSC. For global comparisons of gene expression profiles, we compared 60,675 ENSEMBL genes or (where stated) 19,875 ENSEMBL protein-coding genes expressed at >5 normalized counts in at least one sample. All of the following analysis was carried out in R, using base packages unless stated otherwise.

Hierarchical Clustering of RNA-Seq Transcriptomes (Figure 3A)

Euclidian distances between pairs of $\log_2$-transformed global gene counts were calculated using the R function *dist()* and the distances plotted as a Dendrogram using the *hclust()* function.

Heatmaps (Figures 3B, 3E and 3F)

Heatmaps were plotted using the function *heatmap.2()*.

Specifically Expressed Genes (Figure 3C)

Specifically expressed genes are defined as those with CV > 1 (Coefficient of Variance) and Z-score > 1. CV is defined as the mean divided by the standard deviation across all samples, in this case the aforementioned 23 published tissue datasets plus the cPP and PPd15 gene counts described here. Z-score is defined as the difference between expression in the sample of interest and the mean for all samples, divided by the standard deviation across all samples. When calculating the Z-score for pancreatic samples other pancreatic samples are excluded.

Gene Ontogeny Analysis (Figure 3D)

The web-based gene set analysis tool kit at http://www.webgestalt.org/ was used to analyze Gene Ontogeny (GO) terms associated with genes specifically expressed by cPP cells. Protein-coding genes were ordered according to the product of the coefficient of variance and Z-score for cPP cells (see above) and the top 250 genes selected for enrichment analysis. The Over Representations Analysis (ORA) tool was used to calculate fold-enrichment for biological process GO terms across these 250 genes, using all protein coding genes as the reference set, and the corresponding p-value adjusted by the Benjamini-Hochberg multiple test adjustment. GO terms were ordered according to fold-

enrichment and those associated with < 5 genes and/or an adjusted p-value > 0.01 were eliminated from the enriched set.

In vitro differentiation

Establishing differentiation cultures

Initially, cPP cells were cultured to confluency to eliminate feeder cells then treated with gentle cell dissociation reagent to generate single cells. Single cells were resuspended in cPP culture media + 10 μM Y27632 and seeded according to differentiation platform. To establish 3D sphere cultures, 2 x 10^6 cells were seeded into each well of an ultra low adhesion 6 well plate (Corning, 3471) in 2 mL media and placed on a nutator overnight. Compact spheres typically form after 24 hours. To establish 3D matrigel cultures, AggreWell 400 plates (Stemcell Technologies, 27840) were used to generate spheres of ~200 cells according to the manufacturers instructions. After 24 hours ~1200 spheres were resuspended in 500 μL 1:5-diluted hESC-qualified matrigel (Corning, 354277) and deposited into each well of a 24 well plate. Plates were incubated at 37°C for 60 min to allow matrigel to solidify before addition of media. To establish 2D monolayer cultures, cells were seeded at 6.65 x 10^5 cells/cm^2 on tissue culture plastic coated with matrigel diluted 1:50.

NKX6-1 induction tests

Differentiation cultures were treated with the following signaling regimes, based upon several recently published protocols, with minor alterations (Pagliuca et al., 2014; Rezania et al., 2014; Russ et al., 2015; Zhang et al., 2009). Differentiation media 1 consists of MCDB 131 media (Thermo Fisher Scientific, 10372-01), 2.5 g/L sodium bicarbonate (Lonza, 17-613E), 2 mM L-glutamine, 100 U/mL penicillin/streptomycin, 10 mM glucose (VWR International, 101174Y), and 2% bovine serum albumin (Sigma, A9418). Differentiation media 2 consists of DMEM high glucose, 2 mM L-glutamine, and 100 U/mL penicillin/streptomycin. Media based on PP2 induction media described by Pagliuca et al. consists of differentiation media 1 supplemented with 50 ng/mL FGF7 (R&D Systems, 251-KG), 0.25 mM ascorbic acid (Sigma, A4544), 100 nM RA, 0.25 μM SANT-1 (Sigma, S4572), and 0.5% ITS-X (Thermo Fisher Scientific, 51500056). Media was completely replenished daily for 5 days. Media based on stage 4 media described by Rezania et al. was additionally supplemented with 300 nM Indolactam-V (Stemcell Technologies, 72312) and 200 nM LDN-193189 (Stemcell Technologies,

72142), and was completely replenished daily for 5 days. Media based on day 13-20 media described by Zhang et al. consists of differentiation media 2 supplemented with 10 ng/mL bFGF, 10 mM nicotinamide (Sigma, 24,020-6), 50 ng/mL exendin-4 (Sigma, E7144), 10 ng/mL BMP4 (R&D Systems, 314-BP), and 1% ITS-X. Media was completely replenished daily for 5 days. Media based on day 7-9 media described by Russ et al. consists of differentiation media 2 supplemented with 1X B27 supplement, 50 ng/mL EGF, 1 μM RA (first 24 hours), and 50 ng/mL FGF7 (second 24 hours). Media was completely replenished daily for 2 days.

Quantitative RT-PCR

RNA was isolated from samples using an RNeasy mini kit (Qiagen, cat # 74104) and reverse transcribed to generate cDNA using a high-capacity reverse transcription kit and random hexamer primers (Applied Biosystems, 4368814, 1 μg RNA per 20 μL reaction). Quantitative RT-PCR was carried out using SYBR Select Mastermix (Applied Biosystems, 4472908). Data were analyzed using the ΔΔCT method, and normalized to expression of the housekeeping gene TBP in each sample. The primers used for qRT-PCR are shown in Supplementary Table 3.

Immunofluorescence staining

The following primary antibodies were used for immunofluorescence staining: mouse monoclonal anti-PDX1 (R&D Systems, MAB2419, 1:50), rabbit anti-SOX9 (Sigma, HPA001758, 1:2000), rabbit anti-HNF6 (ONECUT1) (Santa Cruz, SC13050, 1:100), goat anti-FOXA2 (R&D Systems, AF2400, 1:200), rabbit anti-GATA6 (Cell Signaling Technologies, 5851, 1:1600), sheep anti-NGN3 (R&D Systems, AF3444, 1:200), mouse anti-NKX6-1 (developmental studies hybridoma bank, F55A12, 1:80), mouse monoclonal anti-NKX2-2 (BD biosciences, 564731, 1:400), mouse monoclonal anti-pro-Insulin c-peptide (Millipore, 05-1109, 1:100), rabbit monoclonal anti-glucagon (Cell Signaling Technologies, 8233, 1:400), rat monoclonal anti-KRT19 (developmental studies hybridoma bank, TROMA-III-s, 1:10), sheep anti-trypsin (pan-specific) (R&D Systems, AF3586, 1:13). Primary antibodies were recognized by Alexa-fluorophore conjugated secondary antibodies raised in Donkey (Thermo Fisher Scientific, 1:500). Images were acquired using an Olympus FV1000 inverted confocal microscope.

Immunofluorescence staining transplanted kidneys

Mouse kidneys were dissected, cleaned, longitudinally sectioned, embedded in Jung freezing medium (Leica, 020108926), and cryopreserved in liquid nitrogen. Sections (6µm) were mounted on APES-coated glass slides, dried and fixed in 4% paraformaldehyde for 10 min at room temperature. After washing 3X with PBS for 15 min, samples were permeabilised with PBS containing 0.3% Triton X-100 for 10 min, then blocked for 1 hour each in Rodent block M (Biocare medical, RBM961H) and blocking buffer (PBS + 20% normal donkey serum + 1% BSA + 0.3% Triton X-100). After washing 3X with wash buffer (PBS + 0.1% Tween-20 + 0.1% BSA) for 15 min, samples were incubated overnight at 4^{o}C with primary antibodies diluted in blocking buffer. After washing 3X with wash buffer for 15 min, samples were incubated at room temperature for 1 hour with secondary antibodies diluted 1:500 in blocking buffer. All subsequent steps were carried out in the dark. After washing 1X with wash buffer, samples were incubated at room temperature for 20 min with 2µg/mL Hoechst-33342 (Thermo Fisher Scientific, 62249) diluted in PBS. Finally, after washing 3X with wash buffer for 15 min, samples were covered with Vecashield hard set mounting medium (Vector Laboratories, H-1400), covered with a coverslip and sealed.

Immunofluorescence staining cultured cells

Adherent cells were washed 2X with PBS then fixed in 4% paraformaldehyde for 20 min at room temperature. After washing 3X with wash buffer (PBS + 0.1% BSA), samples were incubated with blocking buffer (PBS + 20% normal donkey serum + 0.1% BSA + 0.3% Triton X-100) for 1 hour at room temperature. Samples were then incubated overnight at 4^{o}C with primary antibodies diluted in blocking buffer. After washing 3X with wash buffer for 15 min, samples were incubated at room temperature for 1 hour with secondary antibodies diluted 1:500 in blocking buffer. All subsequent steps were carried out in the dark. After washing 3X with wash buffer for 15 min, samples were incubated at room temperature for 15 min with 2µg/mL Hoechst-33342 (Thermo Fisher Scientific, 62249) diluted in PBS. Finally, samples were washed 2X with PBS for 15 min and imaged.

Immunofluorescence staining differentiation spheres

Differentiation spheres were washed 1X with PBS + 2% serum then fixed in 4% paraformaldehyde for 30 min at room temperature. After washing 1X for 15 min with wash buffer (PBS + 0.1% BSA + 0.1% Tween-20), samples were blocked for 6 hours in blocking buffer (PBS + 20% normal donkey serum + 1% BSA + 0.3% Triton X-100). Samples were then incubated overnight at 4^{o}C with primary antibodies diluted in blocking buffer. After washing 2X with wash buffer for 15 min, samples were incubated at 4^{o}C for 6 hours with secondary antibodies diluted 1:500 in blocking buffer. All subsequent steps were carried out in the dark. After washing 1X with wash buffer for 15 min, samples were incubated at room temperature for 1 hour with 2μg/mL Hoechst-33342 (Thermo Fisher Scientific, 62249) diluted in PBS. Finally, spheres were washed 2X with PBS for 30 min, resuspended in Vectashield hard set mounting medium (Vector Laboratories, H-1400), mounted on glass slides, covered with a coverslip and sealed. All washing and incubation steps are carried out in 1.5mL Eppendorf tubes.

Flow cytometry

Single cells were generated using accutase (Thermo Fisher Scientific, 14190), washed 1X with PBS + 1% serum, then fixed in 4% paraformaldehyde for 10 min at room temperature. Cells were washed 1X with wash/permeabilization buffer (BD, 554723), then up to 10^6 cells were incubated with primary or isotype control antibody diluted in 250μL wash/permeabilization buffer for the required length of time (see below for antibody dilutions and incubation times). For unconjugated antibodies, cells were washed 1X with wash/permeabilization buffer then incubated for 15 min with secondary antibody diluted in wash/permeabilization buffer. If staining for a second antigen, cells were washed 1X with wash/permeabilization buffer then subject to the aforementioned incubation step(s). After washing 1X with wash/permeabilization buffer, cells were resuspend cells in PBS + 1% serum and analyzed using a BD FACSCalibur flow cytometer. All steps were carried out at room temperature and cells were pelleted by centrifugation at 6000 rpm for 5 min in a microcentrifuge.

The following antibodies were used: mouse monoclonal anti-PDX1 PE-conjugate (BD biosciences, 562161, 1:50, 45 min), mouse IgG1 PE-conjugate (BD biosciences, 556650, 1:50, 45 min), mouse monoclonal anti-NKX6.1 (developmental studies hybridoma bank, F55A12, 1:25, 45 min), goat anti-mouse IgG APC-conjugate (BD biosciences, 550828, 1:400, 15 min), mouse monoclonal anti-Oct3/4

Alexa Fluor 488-conjugate (BD biosciences, 560253, 1:5, 60 min), mouse monoclonal anti-pro-Insulin c-peptide (Millipore, 05-1109, 1:100, 60 min), anti-mouse IgG Alexa Fluor 488-conjugate (Thermo Fisher Scientific, A21202, 1:300, 30 min). All flow cytometry experiments were gated using cells stained only with fluorophore-conjugated isotype control (in the case of directly conjugated primary antibodies) or fluorophore-conjugated secondary antibodies.

Microbioreactor Array (MBA) Screening of cPP Maintenance and Proliferation

Microbioreactor arrays (previously described, (Titmarsh et al., 2012)) were used to screen the effects of combinations of exogenous signaling molecules on cPP cells. MBAs provide combinatorial mixing of input factors, combined with continuous flow of culture media over culture chambers. MBAs were autoclaved and filled with sterile PBS, then coated (2-4 h, room temperature) with a single 1 mL injection of hESC-qualified matrigel at the manufacturer's recommended concentration. cPP cells in suspension in complete medium at 5 $\times 10^6$/mL were then seeded in the MBA, giving a surface density of 50×10^6cells/cm^2. Cells were allowed to attach for a total of 20 h, with a media exchange performed every 6 h. Subsequently, factor provision was commenced with an initial filling step of 300μL, followed by constant perfusion of factors at 36 μL/h, for a total culture time of 3 days. At the endpoint, cells were rinsed with PBS, fixed with 2% PFA/PBS solution for 30 min, then rinsed with PBS and blocked/permeabilised with PBS + 20% normal donkey serum + 0.1% BSA + 0.3% Triton X-100 for 30 min. Then, cells were labeled with primary antibodies against PDX1 (R&D Systems, MAB2419, 1:25), and SOX9 (Sigma, HPA001758, 1:1000) diluted in blocking buffer, overnight at 4°C. Cells were then washed with 0.1% BSA/PBS and labeled with Alexa-fluorophore conjugated secondary antibodies (Thermo Fisher Scientific, 1:500 dilution) and Hoechst 33342 (2 μg/mL) for 1 hour. Finally, cells were rinsed with PBS, and the MBA inlets and outlets plugged closed. The MBA was then mounted in a microplate adapter and imaged. Nuclear segmentation and quantification of nuclear intensities of PDX1 and SOX9 then proceeded similarly as previously described (Titmarsh et al., 2016).

Supplementary References

Micallef, S.J., Li, X., Schiesser, J.V., Hirst, C.E., Yu, Q.C., Lim, S.M., Nostro, M.C., Elliott, D.A., Sarangi, F., Harrison, L.C., Keller, G., Elefanty, A.G., Stanley, E.G., 2011. INS GFP/w human embryonic stem cells facilitate isolation of in vitro derived insulin-producing cells. Diabetologia 55, 694–706.

Pagliuca, F.W., Millman, J.R., Gürtler, M., Segel, M., Van Dervort, A., Ryu, J.H., Peterson, Q.P., Greiner, D., Melton, D.A., 2014. Generation of Functional Human Pancreatic b Cells In Vitro. Cell 159, 428–439.

Petryszak, R., Burdett, T., Fiorelli, B., Fonseca, N.A., Gonzalez-Porta, M., Hastings, E., Huber, W., Jupp, S., Keays, M., Kryvych, N., McMurry, J., Marioni, J.C., Malone, J., Megy, K., Rustici, G., Tang, A.Y., Taubert, J., Williams, E., Mannion, O., Parkinson, H.E., Brazma, A., 2013. Expression Atlas update—a database of gene and transcript expression from microarray- and sequencing-based functional genomics experiments. Nucl. Acids Res. 42, D926–D932.

Rezania, A., Bruin, J.E., Arora, P., Rubin, A., Batushansky, I., Asadi, A., O'Dwyer, S., Quiskamp, N., Mojibian, M., Albrecht, T., Yang, Y.H.C., Johnson, J.D., Kieffer, T.J., 2014. Reversal of diabetes with insulin-producing cells derived in vitro from human pluripotent stem cells. Nature Biotechnology.

Russ, H.A., Parent, A.V., Ringler, J.J., Hennings, T.G., Nair, G.G., Shveygert, M., Guo, T., Puri, S., Haataja, L., Cirulli, V., Blelloch, R., Szot, G.L., Arvan, P., Hebrok, M., 2015. Controlled induction of human pancreatic progenitors produces functional beta-like cells in vitro. The EMBO Journal 34, 1759–1772.

Titmarsh, D.M., Glass, N.R., Mills, R.J., Hidalgo, A., Wolvetang, E.J., Porrello, E.R., Hudson, J.E., Cooper-White, J.J., 2016. Induction of Human iPSC-Derived Cardiomyocyte Proliferation Revealed by Combinatorial Screening in High Density Microbioreactor Arrays. Sci. Rep. 1–15.

Zhang, D., Jiang, W., Liu, M., Sui, X., Yin, X., Chen, S., Shi, Y., Deng, H., 2009. Highly efficient differentiation of human ES cells and iPS cells into mature pancreatic insulin-producing cells. Cell Res 19, 429–438.